2018-07-21

Paired dissolved and particulate phase Cu isotope distributions in the South Atlantic

Little, SH

10.1016/j.chemgeo.2018.07.022
Chemical Geology
Elsevier BV

Chemical Geology xxx (xxxx) xxx–xxx

Contents lists available at ScienceDirect

Chemical Geology

journal homepage: www.elsevier.com/locate/chemgeo

VSI: ConwayGEOTRACES

Paired dissolved and particulate phase Cu isotope distributions in the South Atlantic

Susan H. Little[a,*], Corey Archer[b], Angela Milne[c], Christian Schlosser[d,e], Eric P. Achterberg[d,e], Maeve C. Lohan[e], Derek Vance[b]

[a] Department of Earth Science and Engineering, Royal School of Mines, Imperial College London, London SW7 2BP, UK
[b] Institute of Geochemistry and Petrology, Department of Earth Sciences, ETH Zürich, Clausiusstrasse 25, Zürich 8092, Switzerland
[c] School of Geography, Earth and Environmental Sciences, University of Plymouth, Plymouth, PL4 8AA, UK
[d] GEOMAR Helmholtz-Centre for Ocean Research, Kiel, Wischhofstr. 1-3, 24148 Kiel, Germany
[e] Ocean and Earth Sciences, National Oceanography Centre Southampton, University of Southampton, Southampton SO14 3ZH, UK

ARTICLE INFO

Keywords:
Copper isotopes
GEOTRACES
Particulate
Dissolved
South Atlantic

ABSTRACT

Copper (Cu) is both an essential micronutrient and toxic to photosynthesizing microorganisms at low concentrations. Its dissolved vertical distribution in the oceans is unusual, being neither a nutrient-type nor scavenged-type element. This distribution is attributed to biological uptake in the surface ocean with remineralisation at depth, combined with strong organic complexation by dissolved ligands, scavenging onto particles, and benthic sedimentary input. We present coupled dissolved and particulate phase Cu isotope data along the UK-GEOTRACES South Atlantic section, alongside higher resolution dissolved and particulate phase Cu concentration measurements. Our dissolved phase isotope data contribute to an emerging picture of homogeneous deep ocean δ^{65}Cu, at about +0.65‰ (relative to NIST SRM 976). We identify two pools of Cu in the particulate phase: a refractory, lithogenic pool, at about 0‰, and a labile pool accessed via a weak acidic leach, at about +0.4‰. These two pools are comparable to those previously observed in sediments. We observe deviations towards lighter δ^{65}Cu values in the dissolved phase associated with local enrichments in particulate Cu concentrations along the continental slopes, and in the surface ocean. Copper isotopes are thus a sensitive indicator of localised particle-associated benthic or estuarine Cu inputs. The measurement of Cu isotopes in seawater is analytically challenging, and we call for an intercalibration exercise to better evaluate the potential impacts of UV-irradiation, storage time, and different analytical procedures.

1. Introduction

Copper (Cu) is a bioessential element but the free Cu^{2+} ion is toxic at low concentrations (toxicity at $> 10^{-11}$ M), particularly to prokaryotic photosynthesizing bacteria (e.g., Brand et al., 1986). However, aqueous Cu in seawater is predominantly complexed by strong organic ligands, which appear to have a detoxifying influence, as well as retaining Cu in the dissolved phase (e.g., Bruland et al., 2013). Some eukaryotes have higher metabolic Cu requirements than prokaryotes, and may be able to access some portion of the ligand-bound Cu pool (e.g., Semeniuk et al., 2015). The free Cu^{2+} species is particle reactive and readily scavenged by organic and Fe-Mn oxide phases (e.g., Balistrieri et al., 1981; Sherman and Peacock, 2010). In sulphidic solutions, as for example in the Black Sea, Cu exists as the insoluble reduced Cu(I) species CuHS and $Cu(HS)_2^-$ (Mountain and Seward, 1999). This array of behaviours make Cu isotopes a potential target as a (palae-)oceanographic tracer (e.g., Chi Fru et al., 2016), contingent on an understanding of the key processes influencing their modern oceanic cycling.

Recent dissolved and sedimentary solid-phase Cu isotope data have been interpreted in terms of the key role of organic complexation (e.g., Little et al., 2017; Thompson and Ellwood, 2014; Vance et al., 2008), alongside scavenging of the light isotope by particulate material (Little et al., 2014a, 2014b; Takano et al., 2015). To date, however, very little Cu isotope data exists for particulate material in the water column. Particles are a fundamental part of the oceanic biogeochemical cycling of trace metals, both in their input, dissolution, aggregation, disaggregation, and removal to sediments, and as surfaces for scavenging and transport. Isotope data has the potential to distinguish the contribution of, e.g., biogenic, authigenic, and lithogenic phases to the

* Corresponding author.
E-mail address: s.little@imperial.ac.uk (S.H. Little).

https://doi.org/10.1016/j.chemgeo.2018.07.022
Received 1 March 2018; Received in revised form 11 June 2018; Accepted 17 July 2018

total metal complement of the particles in the ocean.

One of the goals of the GEOTRACES program was to address and overcome the difficulties associated with the sampling and analysis of particulate material in the oceans (e.g., Anderson and Hayes, 2015; Lam et al., 2015; Mcdonnell et al., 2015). The result is that high quality trace metal particulate data is now becoming available (e.g., Ohnemus and Lam, 2015; Twining et al., 2015b). Nevertheless, to date, only sparse trace metal isotopic data for marine particles have been presented (e.g., Revels et al., 2015; Thompson and Ellwood, 2014). Maréchal et al. (1999) reported bulk Cu isotope data for six sediment trap samples from the Atlantic. Thompson and Ellwood (2014) reported labile and refractory Cu isotope data for one seawater profile from the Tasman Sea, while acknowledging significant analytical difficulties (Thompson and Ellwood, 2014).

In this study, we present Cu isotope data for two fractions of particulate material (bulk and leachable Cu) collected as part of the UK-GEOTRACES GA10 South Atlantic cruise in 2011–12. We pair this particulate phase isotope data with dissolved phase Cu isotope data from the same sampling stations, and with high resolution dissolved and particulate Cu concentration data from the full GA10 section. The resulting dataset offers new insights into oceanic biogeochemical cycling of Cu, highlighting the role of particulate-associated sources of isotopically light Cu to the dissolved phase.

2. Sampling and analytical methods

All work was carried out under trace metal clean conditions, using acid cleaned Savillex PFA labware except where stated. Deionised water (MilliQ, Millipore, 18.2 MΩ cm) was used throughout, and acids and reagents were either ultrapure or double distilled.

2.1. Sampling methods

Large volume seawater samples for trace metal (Cu, Zn and Ni) isotope analysis at ETH Zürich were collected at six superstations along the South Atlantic UK GEOTRACES GA10 transect (Fig. 1; e.g., Browning et al., 2014, 2017; Tuerena et al., 2015; Wyatt et al., 2014). Three superstations (3, 6 and 11) were occupied during the first cruise, D357, which sailed between 18 October and 22 November 2010 on board the *R.R.S. Discovery*. Three further superstations (12, 18 and 21) were sampled during the second leg, JC068, which took place from 24 December 2011 to 27 January 2012 on the *R.R.S. James Cook*. Higher resolution sampling for trace metal concentration measurements was also carried out along the full GA10 section (Fig. 1). Dissolved Cu concentration data from the second leg (JC068), measured at the National Oceanography Centre Southampton (NOCS), are presented here.

Dissolved phase sampling procedures (for both trace metal concentration and isotope analysis) followed GEOTRACES protocols and are described in Wyatt et al. (2014). In brief, samples were collected using twenty-four 10 L Teflon-coated Niskin (Ocean Test Equipment, OTE) samplers mounted on a titanium CTD frame deployed on a plasma rope. Once on board, samples were filtered through 0.2 µm AcroPak Supor polyethersulfone membrane filter capsules (Pall) into acid-cleaned 0.125, 1 or 4 L low density polyethylene (LDPE) bottles and acidified to pH 1.9 (NOCS) or 1.7 (for isotopes) by addition of 12 M hydrochloric acid (HCl, UpA, Romil).

High resolution bottle sampling for total and leachable particulate trace metal concentrations (University of Plymouth) was carried out along the full GA10 transect using the same twenty-four 10 L OTE samplers. Up to 7 L of seawater was filtered on board through acid washed 25 mm (0.45 µm) PES filters (Pall Gellman) housed in acid clean filter holders (Swinnex, Millipore). Filters were frozen at −20 °C in acid clean 2 mL LDPE vials until analysis.

Particulate phase sampling for Cu isotope analysis at ETH Zürich was carried out using the Challenger Oceanic Stand Alone Pump System (SAPS). The filter houses of the SAPS were fitted with acid-washed nylon mesh (293 mm diameter, 51 µm pore size, Nitex) to collect large fast-sinking particles, and with two stacked 293 mm 0.8 µm polyethersulfone filters (PES, Pall Gelman) to collect < 51 µm fine slow-sinking fraction particles, and deployed to varying depths in the water column. Seawater volumes filtered in situ were in the range ~500–1500 L. Upon removal, the 293 mm PES filters were folded in on themselves and stored frozen at −20 °C in clean zip-lock bags. Subsamples of these < 51 µm fine fraction PES filters from the three JC068 superstations, stations 12 (mid Atlantic ridge), 18 (deep Argentine basin) and 21 (Argentine slope), were analysed for Cu isotopes. Wedges of the large particle size fraction (> 51 µm) nylon filters were rinsed with deionised water and the particles re-collected on a 25 mm PES filter, which were subsequently digested following the same protocol as the bottle collected particles at the University of Plymouth (see Section 2.3).

2.2. Analysis of dissolved Cu

2.2.1. High-resolution dissolved Cu concentrations at NOC Southampton

High-resolution Cu concentration analyses for all samples from the JC068 cruise were made at NOCS, following Rapp et al. (2017). In brief, acidified seawater aliquots were spiked with a multi-element standard of trace metal isotopes enriched over natural abundance (including ^{65}Cu) and UV-irradiated for 4 h prior to solid-phase extraction. Trace metals were then pre-concentrated using an automated system (Preplab, PS Analytical) equipped with a WAKO chelating resin (similar to Presep ® Polychelate, WAKO Pure Chemical Industries, Japan), with immobilized carboxymethylated pentaethylenehexamine (CM-PEHA) functional groups (Kagaya et al., 2009). Trace metals were eluted with 1 M sub-boiled HNO_3 and analysed using a Thermo Element XR in medium resolution mode.

The accuracy and precision of the method was validated by analysis of the SAFe seawater reference standards D2 and S. Results are presented in Table 1. The precision for replicate analyses was between 1

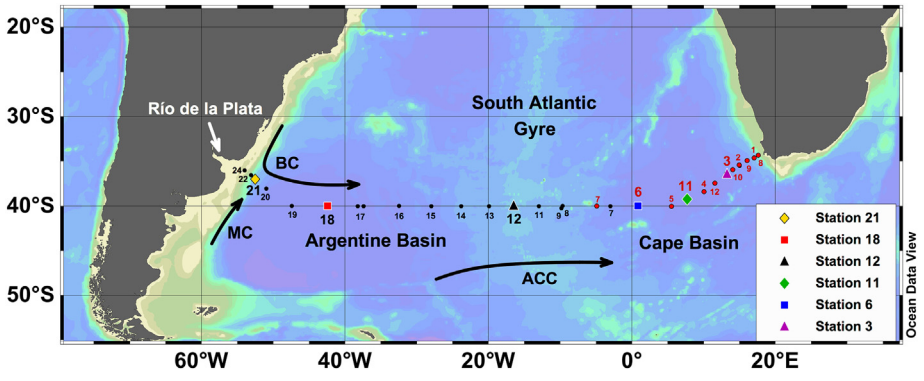

Map made using Ocean Data View (Schlitzer, 2016).

Fig. 1. Map of UK GEOTRACES South Atlantic GA10 section showing occupied stations and superstations and relevant ocean currents. Stations in red, in the Cape Basin, were occupied during cruise leg D357 (Oct–Nov 2010). This leg included superstations 3, 6 and 11, for which dissolved phase Cu isotope data are reported here. Stations in black were occupied during cruise leg JC068 in the Argentine Basin (Dec 2011–Jan 2012), during which three superstations (12, 18 and 21) were sampled for dissolved and particulate phase Cu isotope data. Stations 1–3 were also reoccupied during this later cruise. (For interpretation of the references to colour in this figure legend, the reader is referred to the web version of this article.)

Table 1
SAFe reference seawater samples analysed for dissolved Cu concentrations at NOC Southampton.

Reference Seawater	Cu (nmol kg^{-1})	s.d.
SAFe D2	2.15	0.16
Consensus	2.25	0.11
n =	22	
SAFe S	0.55	0.06
Consensus	0.51	0.05
n =	30	

Detection Limit: 0.011 nmol kg^{-1}.
Procedural Blank: 0.019 nmol kg^{-1}.

and 3%. The manifold blank (from the preconcentration procedure) was neglectable, while the buffer blank (NH_4Ac) was 0.019 ± 0.005 (σ_{bl}) nmol Cu L^{-1} (see Rapp et al., 2017 for details). The limit of detection (3 × standard deviation of the blank) was determined as 0.011 ± 0.005 (σ_{bl}) nmol Cu L^{-1}.

2.2.2. Dissolved Cu isotopes at ETH Zürich

For Cu isotope analysis at ETH Zürich, dissolved phase Cu samples from the six superstations were preconcentrated using a method adapted from Takano et al. (2013), described in Vance et al. (2016). Briefly, trace metals (including Cu) were preconcentrated from 0.2–4 L seawater samples using Nobias chelate PA-1 resin (Hitachi High Technologies, Sohrin et al., 2008; Takano et al., 2013) held in a PFA Teflon cartridge. Metals were then eluted from the resin with 1 M HNO_3. The eluate was evaporated to dryness and redissolved in 7 M HCl for subsequent Cu purification by column chromatography (see Section 2.4).

Procedural blanks were measured numerous times by passing various volumes of deionised water through the entire procedure, with the resultant blanks then measured on the Element XR. These procedural blanks were consistently < 0.5 ng Cu. Recovery tests were carried out using samples of surface Sargasso Sea water (presumed to have very low trace metal concentrations). In separate experiments 200 and 750 ng/L of NIST Cu respectively was added to two seawater aliquots and allowed to equilibrate for 24 h. Each aliquot was split into five subaliquots from which the Cu was then pre-concentrated and purified as detailed here. Recovered Cu was 96–115% for the two experiments, with δ^{65}Cu = 0.03 ± 0.07‰ (2 SD). Full duplicate analyses were also carried out for two samples (JC068 1952 and D357 767, Table 3).

Dissolved phase samples for isotope analysis were not subjected to UV oxidation prior to preconcentration. However, they were stored, acidified, for ≥4 years prior to analysis. This duration is considered sufficient to lead to degradation of the naturally present complexing organic ligands, and thus allow complete Cu extraction by the added chelating resin (Posacka et al., 2017). Consistent with this suggestion, we observed reasonable agreement between Cu concentrations from the isotope analysis (obtained from beam matching with standards of known concentration) with the more precise data produced via isotope dilution (Fig. 2). For a more detailed discussion of the analytical challenges associated with the measurement of Cu and Cu isotopes in seawater, see Section 4.1.

2.3. Analysis of total and leachable particulate Cu

Particulate samples for concentration measurements only (Univ. Plymouth) and for concentration and isotopic analysis (ETH Zürich) were subject to different leach and bulk digestion procedures, detailed below.

2.3.1. Bulk and leachable particulate Cu isotopes at ETH Zürich

For Cu isotope analysis, the fine fraction (< 51 µm) 293 mm PES filter membranes (from SAPS) were subsampled using an acid-leached ceramic blade. 1/16th of each filter was bulk digested by ashing (High

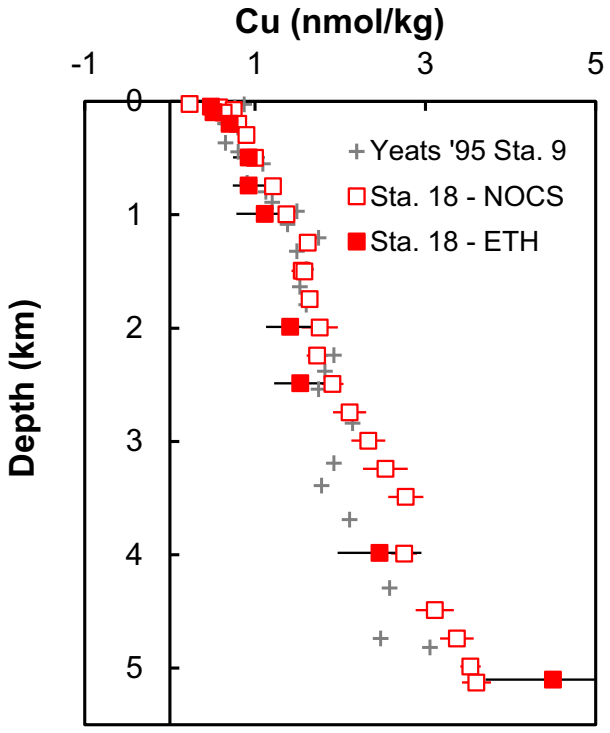

Fig. 2. Comparison of dissolved phase Cu concentration data for Station 18 produced by isotope dilution + UV irradiation (open squares, NOC Southampton) and after preconcentration without UV irradiation by Nobias following ~4 years acidification (filled squares, ETH Zürich). Uncertainty (error bars) on ETH dissolved concentrations is estimated at ± 20%.
For reference, an example of previously published data from the South Atlantic is shown in grey (grey pluses (+): Station 9, Yeats et al. (1995)

Pressure Asher, HPA Anton Paar) in 5 mL concentrated HNO_3. These bulk digests were then evaporated and treated twice with 1 mL concentrated HNO_3 and once with 1 mL concentrated HCl to remove residual H_2SO_4 (present from digestion of the PES filter). A further 1/16th of each filter was subject to a 16 h leach in 30 mL 0.6 M HCl at 65 °C, following Bishop and Wood (2008). This latter methodology aims to liberate the labile metal fraction. Bulk digests and leachable Cu fractions were then evaporated and redissolved in 2% HNO_3. An aliquot of these solutions was taken for multi-element concentration analysis using a Thermo Element XR at ETH Zürich.

Procedural blanks for particulate trace element analyses are challenging to assess and counteract (e.g., Planquette and Sherrell, 2012; Twining et al., 2015a). Here, they were estimated in three ways (Table 2). First, procedural ashing and 0.6 M HCl leaching blanks were measured. Second, acid-cleaned, unused PES filters were subject to the bulk digest (ashing) and leaching procedures. These unused filter blanks were low, at 0.4 and 1.2 ng (per total 47 mm filter) for leaching and digestion respectively (up to a maximum of 3 and 5% of sample Cu contents), and they were similar in magnitude to the (filter-free) ashing

Table 2
Estimates of procedural blanks for particulate Cu, ETH Zürich.

Blank type	Cu (ng)	δ^{65}Cu (‰)
Asher blanks (in duplicate)	1.4, 0.2	nd
0.6 M HCl leach blanks (in duplicate)	0.6, 1.9	nd
Unused 47 mm PES filters, Ash	1.2 ± 0.8 (n = 8)	nd
Unused 47 mm PES filters, 0.6 M HCl leach	0.4 ± 0.2 (n = 8)	nd
Dipped blanks, Ash	*20.1*, 10.1	*0.04 ± 0.06*
Dipped blanks, 0.6 M HCl leach	*14.2*, 9.5	*−0.03 ± 0.06*

nb. Isotope analyses refer to italicised dipped blank values.

and leaching blanks (Table 2). Third, two so-called 'dipped blanks' were recovered and analysed (range: 9–20 ng). These dipped blanks went through the full shipboard procedure but the SAPS pumps failed, and < 6 L of seawater was filtered.

We consider the dipped blanks to be a conservative estimate of the total procedural blank. Both originate from deep waters (Station 18–5000 m, and Station 12–2590 m), with high dissolved Cu concentrations. Previous work suggests flow-dependent adsorption of Cu can occur on filter membranes, which may lead to artefacts (Planquette and Sherrell, 2012). Deep Station 18 is also situated in a region of very elevated particulate Cu concentrations. At Station 12, the coarse size fraction particulates (> 51 µm, Nitex filters) exhibited variable and high Fe/Al ratios (data not shown) and Cu concentrations (Table S1), indicating contamination (see also Section 3.2). Isotopically, the one dipped blank analysed for leachable particulate δ^{65}Cu (at −0.03‰, Table 2) is markedly different to the homogeneous dataset obtained for samples (at +0.40 ± 0.10‰, n = 16, 1 SD; Section 3.2). Given these rather limited constraints on the 'true' total procedural blank, and because filter blank Cu contents were too low to measure for δ^{65}Cu, we do not make a blank-correction to the particulate phase isotope data. Instead, we keep in mind that any blank likely introduced a bias towards isotopically lighter δ^{65}Cu values.

2.3.2. High-resolution particulate Cu concentrations at University of Plymouth

At the University of Plymouth, the bottle filtration 0.45 µm, 25 mm PES filters were acid digested for total particulate Cu concentrations (TpCu) following the Pirahna method of Ohnemus et al. (2014). Briefly, this method involves refluxing the filters in H_2SO_4 + H_2O_2 at 235 °C and evaporation to dryness, followed by refluxing in 4 M HF/HCl/HNO_3 at 135 °C overnight and evaporation again to dryness, with a final stage in concentrated HNO_3 and H_2O_2 at 130 °C before final evaporation to dryness.

Also at the University of Plymouth, selected 25 mm filters from bottle filtration were subjected to a leach (prior to total digestion) following a similar method to that of Berger et al. (2008). A 2 h leach, including 30 min of heating at 90 °C, was carried out in 25% acetic acid plus the reducing agent hydroxylamine hydrochloride (0.02 M). After a 2 h contact time, the filters were removed and placed into digestion vials. The leachate solution was then centrifuged at 3500*g* for 15 min. Following centrifugation, 1 mL of the leachate was transferred to a clean leach vial and evaporated to dryness. Any particles collected during centrifugation were transferred with H_2O_2 to the relevant total particulate digestion vial. These data are referred to as leachable particulate Cu (LpCu) concentrations.

All TpCu and LpCu samples were then redissolved in 2% HNO_3 for ICP-MS analysis. In/Ir and Rh were used as internal standards, and an external calibration was used with mixed element standards ranging from 0.1 to 500 ppb. Analysis was carried out on a Thermo Element X Series 2 equipped with a collision cell utilising 7% H in He at the University of Plymouth. The efficiency of the digestion procedure was assessed using certified reference materials BCR-414 (Trace elements in plankton; Institute for Reference Materials and Measurements), LKSD-4 (lake sediment; Natural Resources Canada) and IAEA-433 (marine sediment; International Atomic Energy Agency), with the determined Cu data in good agreement with the certified values (Table S2).

Both LpCu and TpCu concentrations were blank corrected with values obtained from replicate analyses of unused filters. These filters had been acid washed, stored and processed in the same manner as those used for particle sample collection. The subsequent blank deductions (leach - 0.32 ± 0.1 ng, n = 15; digestion - 0.52 ± 0.1 ng, n = 32) include any contribution from the 25 mm PES filter, the reagents used and the instrumental background.

2.4. Cu isotope analysis

Purification of the Cu fraction of both the dissolved and particulate samples for isotope analysis followed a previously published two-pass anion-exchange procedure using AG MP-1M resin (BioRad; after Archer and Vance, 2004; Little et al., 2014b; Maréchal et al., 1999). Isotope analyses were made on a Neptune Plus MC-ICP-MS at ETH Zürich in low-resolution mode, with introduction via a Savillex C-Flow PFA nebuliser (50 µL min^{-1}) attached to a glass spray chamber (details in Little et al., 2017). Very stable instrumental mass bias allows for high precision instrumental mass fractionation correction using a sample-standard bracketing procedure with untreated normalising standard, NIST SRM 976. Isotope values are reported in delta-notation relative to this standard:

$$\delta^{65}Cu = 1000\left[\frac{(^{65}Cu/^{63}Cu)_{sample}}{(^{65}Cu/^{63}Cu)_{SRM976}} - 1\right]$$

Sodium (Na) concentrations in the final solutions were monitored, and Na-doped standards were run alongside the sample measurements. Minor corrections were made for six particulate samples with residual Na, but these corrections did not exceed 0.03‰. The long-term reproducibility of a secondary pure Cu standard over the period of these measurements was δ^{65}Cu = +0.11 ± 0.06‰ (n = 112, 2 SD), compared to +0.10 ± 0.06‰ measured at the Hebrew University (Asael et al., 2007).

3. Results

3.1. The dissolved distribution of Cu and δ^{65}Cu

The concentration of dissolved Cu in the South Atlantic shows the familiar near linear increase with depth (Figs. 3 and 4), consistent with previously published observations (e.g., Boyle, 1981; Boyle et al., 1977; Bruland and Franks, 1983; Jacquot and Moffett, 2015; Roshan and Wu, 2015). Near surface Cu concentrations are ~0.5 nM and increase to a maximum of 3 to 3.5 nM at abyssal depths. Deep-water concentrations are slightly greater in the Argentine Basin than the Cape Basin, as also observed for dissolved macronutrients, e.g., silicate (Fig. 4; Wyatt et al., 2014).

Dissolved phase Cu isotope values are, for the most part, homogeneous across the basin (Figs. 3 and 5; Table 3). Excluding two outliers the South Atlantic Cu isotope composition is +0.64 ± 0.09‰ (n = 61, 1 SD) or, below 200 m water depth, $\delta^{65}Cu_{>200\ m}$ = +0.66 ± 0.07‰ (n = 39, 1 SD). The two outliers are isotopically heavy (at +0.94 and + 0.99‰, both > 3 SD away from the mean value) and are difficult to interpret. One sample (ID# 170, +0.99‰) from Station 3, 594 m, is close to the South African margin. Other moderately heavy δ^{65}Cu values (at about +0.8‰) are observed through the upper 2000 m of the water column at this station (Fig. 3). These values may indicate a different source of Cu along this margin, e.g., isotopically heavy Cu associated with the Aghulas current, which brings warm, salty water from the Indian Ocean into the southeastern Atlantic (e.g., Paul et al., 2015). The second outlier (ID# 434, +0.94‰, Station 6, 1000 m) is more difficult to explain, and both outliers may, in fact, represent contamination. In the absence of more published supporting data (e.g., dissolved Fe, Fe isotopes) from the GA10 section, these two samples are not discussed further here.

Deviations towards isotopically lighter δ^{65}Cu (at +0.4 to +0.5‰) are observed in surface waters at stations 21 and 18 and in the subsurface at stations 12 and 6 (Fig. 3). Smaller deviations towards lighter δ^{65}Cu are also present close to the continental margins along both the western Argentine Slope (at ~1500 m and > 3000 m) and deep eastern Cape Basin (at > 4000 m) (Fig. 5). These margin-associated light isotope signatures are within one-two standard deviations of the deep basin δ^{65}Cu mean. However, enrichments in total (and leachable)

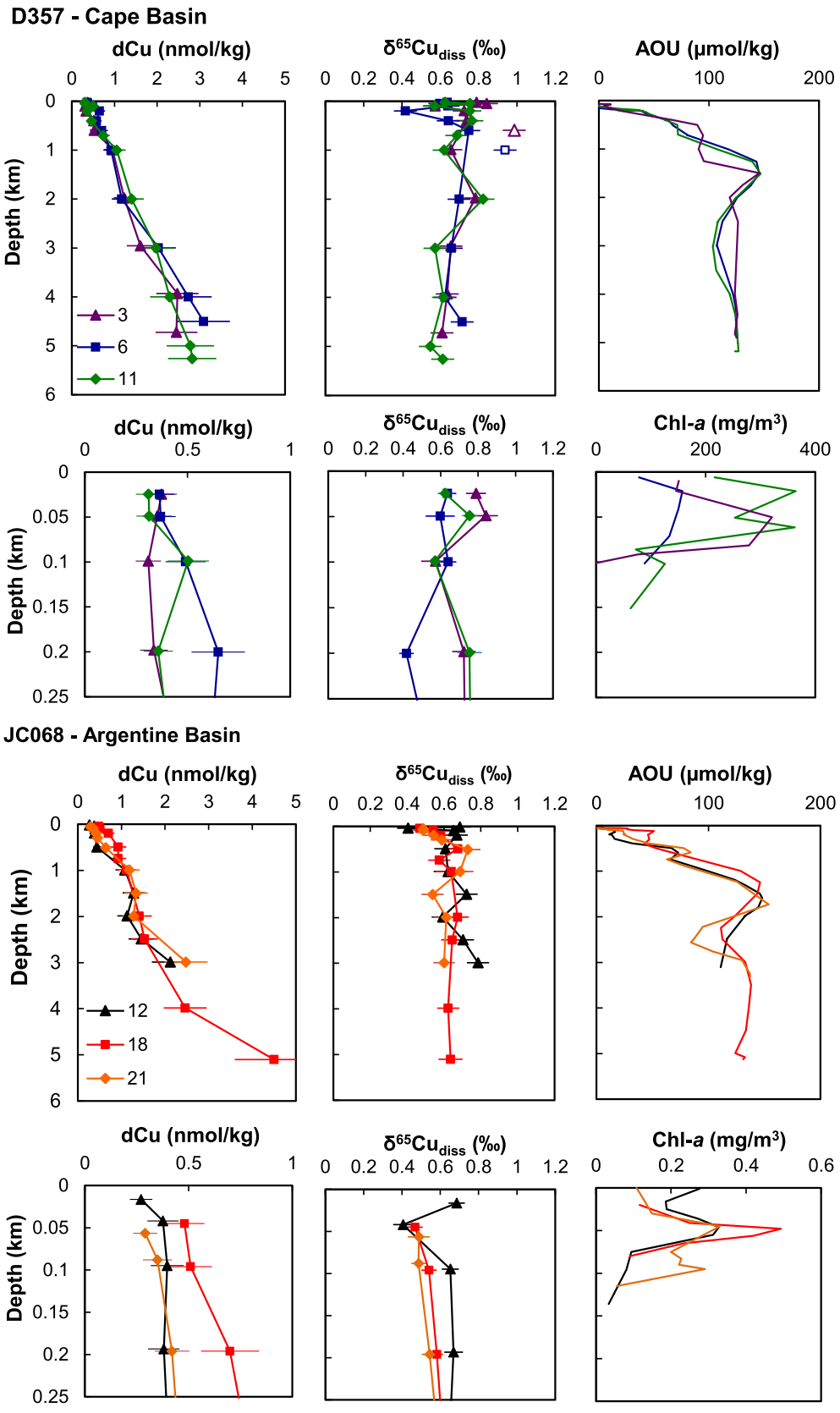

Fig. 3. Dissolved phase Cu concentration (dCu) and isotope data ($\delta^{65}Cu_{diss}$) for the six superstations from the two cruise legs (D357 – Cape Basin and JC068 – Argentine Basin) of the GA10 section. Uncertainty (error bars) on dissolved concentrations is estimated at ± 20% and on isotope values is given as the long-term reproducibility of a secondary standard (± 0.06‰) or internal 2-sigma (where the latter is larger). Full depth profiles are compared to AOU (Wyatt et al., 2014), while upper water column (upper 200 m) zooms are compared to chlorophyll-*a* concentrations (Wyatt et al., 2014). Note very high Chl-*a* concentrations in the Cape Basin (D357 stations) compared to the Argentine Basin (JC068 stations). Two isotopically heavy outliers are shown in the open symbols (see text for discussion).

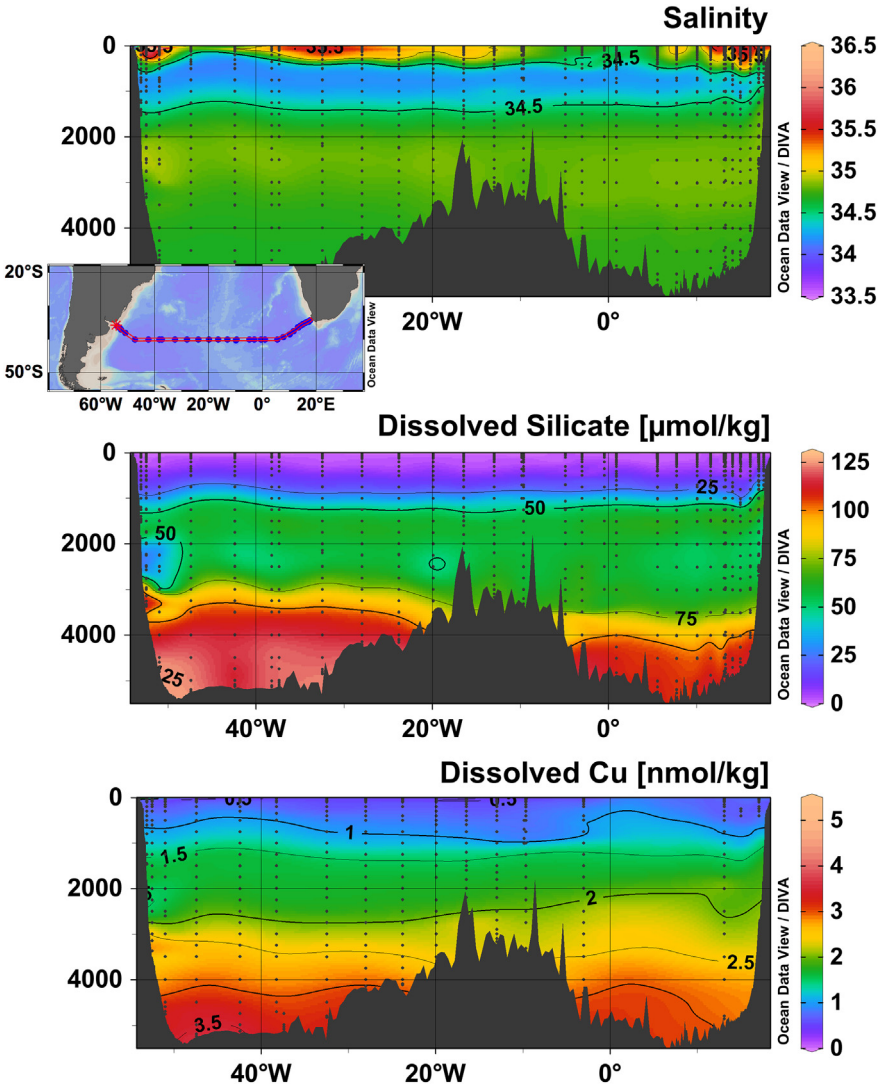

Fig. 4. Sections along GA10: Salinity and dissolved silicate from Wyatt et al. (2014); dissolved Cu concentrations by isotope dilution (NOC Southampton). Plots made using Ocean Data View (Schlitzer, 2016).

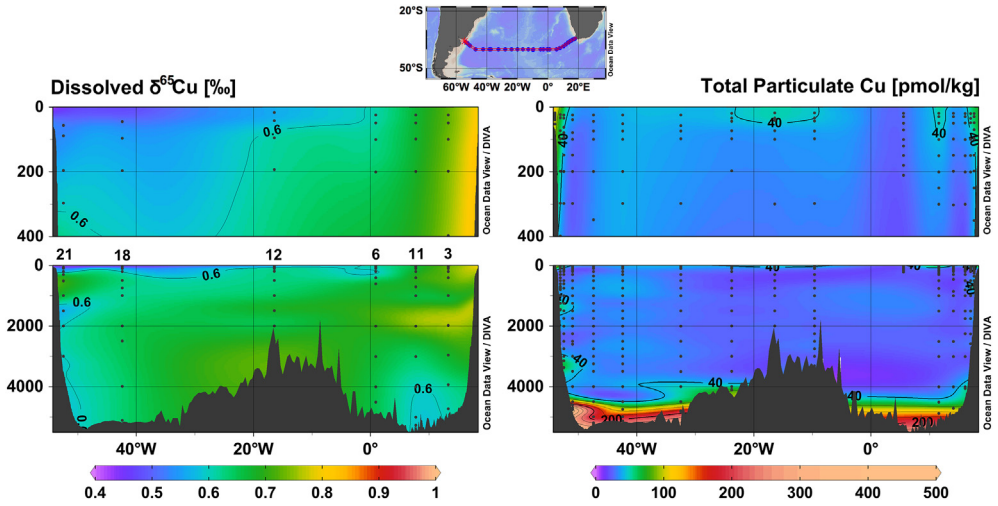

Fig. 5. Sections along GA10: dissolved Cu isotopes (ETH Zürich); total particulate Cu concentrations (bottle filtration, Univ. Plymouth). Plots made using Ocean Data View (Schlitzer, 2016).

Table 3
Dissolved Cu and δ^{65}Cu values for the six superstations of GA10.

Cruise/Station	Sample ID	Water Depth (kM)	Cu (nmol kg^{-1})	± 20%	δ^{65}Cu (‰)	2 sigma[a]
JC068 – Argentine Basin						
Station 12	1560	0.016	0.27	0.05	0.69	0.06
	1555	0.042	0.38	0.08	0.41	0.06
	1551	0.095	0.40	0.08	0.65	0.06
	1547	0.193	0.38	0.08	0.67	0.06
	1517	0.492	0.44	0.09	0.61	0.06
	1513	0.990	1.08	0.22	0.62	0.08
	1509	1.488	1.28	0.26	0.72	0.06
	1505	1.987	1.13	0.23	0.59	0.06
	1502	2.487	1.45	0.29	0.70	0.06
	1498	2.988	2.12	0.42	0.78	0.06
Station 18	2019	0.045	0.48	0.10	0.47	0.06
	2013	0.096	0.51	0.10	0.54	0.06
	2010	0.196	0.7	0.14	0.58	0.06
	2007	0.494	0.93	0.19	0.68	0.07
	2004	0.742	0.92	0.18	0.57	0.06
	2002	0.992	1.12[b]	0.33[b]	0.64	0.08
	1972	1.990	1.41	0.28	0.67	0.06
	1969	2.488	1.53	0.31	0.64	0.06
	1962	3.983	2.46	0.49	0.62	0.06
	1952	5.102	3.97	0.79	0.66	0.06
	1952rep	5.102	5.03	1.01	0.61	0.06
Station 21	2328	0.057	0.29	0.06	0.49	0.06
	2322	0.088	0.35	0.07	0.49	0.06
	2316	0.196	0.42	0.08	0.54	0.06
	2313	0.296	0.45	0.09	0.59	0.06
	2311	0.510	0.64	0.13	0.73	0.07
	2282	0.992	1.18	0.24	0.69	0.07
	2279	1.492	1.34	0.27	0.54	0.06
	2275	1.993	1.28	0.26	0.61	0.07
	2268	2.987	2.48	0.50	0.60	0.06
D357 – Cape Basin						
Station 3	0183	0.025	0.37	0.07	0.79	0.06
	0180	0.049	0.35	0.07	0.84	0.06
	0177	0.099	0.31	0.06	0.57	0.06
	0174	0.198	0.34	0.07	0.72	0.06
	0171	0.397	0.52	0.10	0.74	0.06
	0170	0.594	0.53	0.11	*0.99*[c]	*0.06*
	0169	0.989	0.95	0.19	0.65	0.06
	0167	1.975	1.23	0.25	0.78	0.06
	0166	2.955	1.61	0.32	0.66	0.06
	0164	3.931	2.48	0.50	0.64	0.06
	0163	4.724	2.45	0.49	0.61	0.06
Station 6	0448	0.025	0.36	0.07	0.64	0.06
	0445	0.049	0.37	0.07	0.60	0.06
	0442	0.100	0.49	0.10	0.64	0.06
	0439	0.200	0.65	0.13	0.42	0.06
	0436	0.401	0.58	0.12	0.64	0.06
	0435	0.600	0.70	0.14	0.75	0.06
	0434	0.998	0.92	0.18	*0.94*[c]	*0.06*
	0432	1.999	1.17	0.23	0.70	0.06
	0431	2.998	2.03	0.20	0.66	0.06
	0429	4.000	2.73	0.27	0.62	0.06
	0428	4.501	3.09[b]	0.93[b]	0.71	0.06
Station 11	0785	0.025	0.31	0.06	0.62	0.06
	0782	0.049	0.31	0.06	0.75	0.06
	0779	0.099	0.50	0.10	0.57	0.06
	0776	0.199	0.36	0.07	0.75	0.06
	0773	0.401	0.46	0.09	0.76	0.06
	0772	0.700	0.74	0.15	0.69	0.06
	0771	1.000	1.05	0.21	0.62	0.06
	0769	1.999	1.40	0.28	0.82	0.06
	0768	2.999	1.98	0.40	0.57	0.06
	0767	4.000	2.49	0.50	0.60	0.06
	0767rep	4.000	2.10	0.42	0.63	0.06
	0766	5.000	2.78	0.56	0.55	0.06
	0764	5.260	2.82	0.56	0.61	0.06

[a] External long-term reproducibility of a secondary standard (2 SD) or internal 2 sigma where the latter is larger.
[b] Spilt Cu fraction, Cu concentrations estimated.
[c] Italicised Cu isotope values are anomalous, see text for discussion.

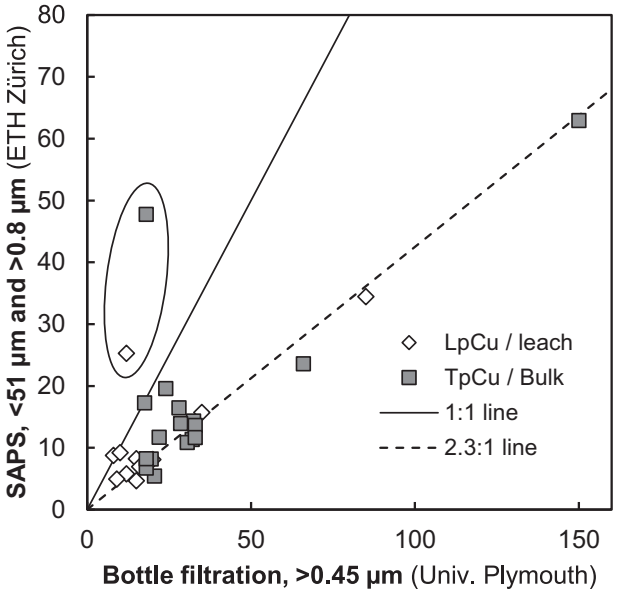

Fig. 6. Comparison of total or bulk and leachable particulate Cu concentrations from the two different sampling procedures, by SAPS (fine-fraction, < 51 µm) using 0.8 µm PES filters (measured at ETH Zürich) and by bottle filtration using 0.45 µm PES filters (measured at Univ. Plymouth). Fine-fraction SAPS concentrations are consistently a factor ~2.3 lower than those from bottle filtration, for both total or bulk and leachable particulate Cu. One anomalous sample is circled (see text for discussion). Note: not all samples are from precisely the same sampling depths.

particulate Cu concentrations are observed at the same depths (Section 3.2, Fig. 5), adding some confidence to their actuality. The deepest sample at Station 12 (at 2988 m, overlying the Mid-Atlantic Ridge (MAR)) is slightly isotopically heavy, at +0.78‰, compared to the average South Atlantic δ^{65}Cu value (Fig. 3).

3.2. Particulate Cu and δ^{65}Cu

Fig. 6 compares particulate Cu concentrations from the two different sampling procedures, i.e., small size-fraction (< 51 µm) SAPS filtration (293 mm 0.8 µm PES filters) versus bottle filtration (25 mm 0.45 µm PES filters), for samples from the same or similar depths. Where possible, both total or bulk and leachable particulate Cu data are compared. Note: leaching procedures also differed between the two laboratories (Section 2.3). With the exception of one sample (circled – see below), fine size fraction SAPS Cu concentrations measured at ETH Zürich are consistently a factor ~2.3 lower than those from bottle filtration (Univ. Plymouth), for both total/bulk and leachable particulate Cu concentrations (Fig. 6). This offset primarily reflects the use of 51 µm nylon mesh (Nitex) pre-filters, which remove the large, fast-sinking particle size fraction prior to the 0.8 µm PES filter on the SAPS.

Summed coarse (Nitex, > 51 µm) and fine (< 51 µm, > 0.8 µm) size fraction pCu concentrations from SAPS give TpCu values comparable to those from bottle filtration (Fig. S1, Table S1). Excluding the aforementioned outlier, TpCu from SAPS are on average 8 ± 13pM (1 SD) lower than TpCu values from bottle filtration, with some scatter in the relationship due to the mismatched sampling depths for SAPS and bottle filtration. The residual small offset may be due to the larger pore size of the SAPS PES filter membranes (0.8 µm cf. 0.45 µm for bottle filtration), which may lead to less efficient collection of the smaller cells (i.e. picophytoplankton and bacteria < 1 µm) that dominate in the subtropical gyres and at depth (Twining et al., 2015a).

The anomalous sample circled on Fig. 6 is the deepest SAPS sample from station 12. The coarse size fraction pCu (from Nitex filter) for this sample is also very high (an order of magnitude higher than any other sample; Table S1). The operator noted the presence of numerous copepods on the outside of the SAPS pumps from greater depth at Station 12. It is likely, therefore, that the elevated bulk and leachable SAPS pCu concentrations for this sample (compared to bottle filtration data) reflect contamination. This SAPS sample and its isotopic signature are therefore considered anomalous and are not discussed further.

Overall, the pCu concentration pattern with depth is similar for bulk and leachable Cu from bottle filtration and from smaller size fraction SAPS, albeit that the latter concentrations are a factor ~2.3 lower. This similarity indicates that, in general, the fine size fraction SAPS samples are representative of the total particulate material present. In addition, the choice of leaching procedure does not appear to be critical.

High-resolution total particulate Cu (TpCu) concentrations, obtained from bottle filtration, are illustrated in section view in Fig. 5. TpCu concentrations are low (< 30 pM) and homogeneous throughout the ocean interior, with significantly elevated values (> 50 pM, maximum value 497 pM) present at depths > 4000 m in the abyssal plains of the deep Argentine and Cape Basins. Notable enrichments (> 50 pM) are also observed along the western Argentine slope at ~1500 m and 3000–3500 m water depth and on the eastern Cape slope at ~700 m water depth (Fig. 5). More subtle surface water TpCu enrichments (range: 29 pM–192 pM) are also observed across the whole section, particularly close to the Argentine margin (Fig. 5). The leachable particulate Cu (LpCu) distribution is very similar, with LpCu concentrations on average 56 ± 11% (n = 112, 1 SD) of TpCu concentrations (Fig. S2).

At the three superstations for which we have the fine size fraction (SAPS < 51 µm) particulate phase Cu isotope data from SAPS, bulk pCu concentrations are homogeneous at 12.1 ± 4.1 pM (n = 14, 1 SD), excluding the deepest samples of each station, which are enriched (Table 4, Fig. 7). This deep enrichment is consistent with observations from bottle filtration data. Leachable particulate Cu concentrations from the < 51 µm SAPS filters, excluding the bottommost samples, are 6.2 ± 2.0 pM (n = 14, 1 SD; Fig. 7). As observed for bottle filtration, leachable pCu concentrations are approximately 50% of bulk pCu concentrations.

Fine size fraction bulk and leachable pCu isotope values are isotopically light (at −0.03‰ to +0.54‰) relative to the mean South Atlantic dissolved seawater value (at +0.64 ± 0.09‰). Leachable pCu isotope values are homogeneous with depth, at +0.40 ± 0.10‰ (n = 16, 1 SD; Fig. 7). Bulk pCu isotope values shallower than ~150 m are isotopically similar to this labile pool (at +0.33 ± 0.10‰, n = 6, 1SD; Fig. 7). Bulk pCu isotope values deeper than 150 m are isotopically lighter, at +0.11 ± 0.09‰ (n = 10, 1 SD; Fig. 7), and similar to the average lithogenic Cu isotope composition (at +0.08 ± 0.17‰, n = 334, 1 SD; Moynier et al., 2017).

4. Discussion

4.1. Analytical challenges associated with dissolved Cu and δ^{65}Cu: a call for intercalibration

The specific challenges associated with the Cu concentration and δ^{65}Cu datasets presented here merit a short discussion prior to their interpretation.

Firstly, measurement of δ^{65}Cu in any sample matrix is analytically difficult. The application of a double spike technique to correct for mass fractionation during sample preparation or mass spectrometry is not possible, because Cu only has two stable isotopes (abundances: ^{63}Cu ~69%, ^{65}Cu ~31%). As a result, Cu yields during sample digestion or pre-concentration and purification must be ~100% (e.g., Maréchal and Albarède, 2002). Instrumental mass fractionation is then corrected via either sample-standard bracketing or elemental doping with Zn or Ni (e.g., Archer and Vance, 2004; Bermin et al., 2006; Ehrlich et al., 2004; Larner et al., 2011; Maréchal et al., 1999; Mason et al., 2005; Vance et al., 2008; Zhu et al., 2002). Sample-standard bracketing, while

Table 4
Fine fraction (< 51 μm, > 0.8 μm, from SAPS) particulate Cu concentrations and δ^{65}Cu values for the three superstations from JC068 cruise along GA10 (the Argentine Basin). Leachable (weak acidic leach, see text for details) and bulk (total digest by ashing) values are given.

Station	Water depth (kM)	Volume (L)	Leachable Cu						Bulk Cu (by ashing)					
			Cu (pM)	Cu/Al ($\times 10^{-4}$)	Cu/Mn	Cu/P	δ^{65}Cu (‰)	2 sigma	Cu (pM)	Cu/Al ($\times 10^{-4}$)	Cu/Mn	Cu/P	δ^{65}Cu (‰)	2 sigma
21	0.1	719	4.9	62.7	0.079	1.2	0.37	0.07	8.2	38.5	0.1	1.7	0.37	0.06
	0.15	1128	3.3	65.1	0.078	2.1	0.56	0.12	6.7	14.7	0.1	3.4	0.43	0.06
	0.25	1250	4.3	26.7	0.024	8.2	0.41	0.06	8.2	4.1	0.0	7.3	0.12	0.06
	0.4	1562	2.9	7.3	0.030	11.5	0.45	0.06	5.4	1.6	0.1	13.0	0.25	0.06
	1	870	6.1	12.8	0.135	30.9	0.53	0.06	11.7	3.4	0.2	28.5	0.17	0.06
	2.6	540	6.9	8.7	0.072	47.4	0.33	0.06	10.9	2.4	0.1	35.7	0.05	0.06
	3.26	949	15.7	5.7	0.082	61.2	0.47	0.06	23.6	1.5	0.1	36.2	0.13	0.06
18	0.05	445	8.1	281.8	0.350	0.5	0.32	0.08	13.6	87.6	0.5	0.7	0.38	0.06
	0.15	899	5.8	23.4	0.094	7.1	0.34	0.06	13.9	4.5	0.2	8.1	0.15	0.06
	0.25	947	6.8	20.2	0.180	9.6	0.48	0.06	14.3	3.9	0.3	11.0	0.05	0.06
	4.9	530	34.4	5.0	0.057	89.1	0.21	0.06	62.9	1.6	0.1	64.5	0.03	0.06
12	0.06	873	9.2	59.0	0.503	1.2	0.48	0.06	19.6	41.2	0.7	1.7	0.37	0.06
	0.15	1123	4.7	79.5	0.097	3.7	0.54	0.06	11.4	35.3	0.2	5.7	0.27	0.06
	0.4	506	8.7	67.9	0.076	9.9	0.39	0.06	17.3	32.4	0.1	10.8	0.24	0.06
	0.975	730	6.8	62.5	0.158	38.5	nd	nd	11.7	23.2	0.2	38.6	0.11	0.06
	2.84	543	8.2	24.5	0.286	51.1	0.27	0.06	16.5	13.4	0.4	50.4	−0.03	0.06
	2.99	898	*25.3*	*89.4*	*0.694*	*218.4*	*0.21*	*0.06*	*47.8*	*37.1*	*0.9*	*218.9*	*−0.08*	*0.06*
Dipped blank	2.59	6					0.04	0.06					0.01	0.06

Italicised samples believed to be contaminated based on comparison with bottle filtration data. See text for discussion.

straightforward, is subject to minor residual matrix effects, while elemental doping assumes that the mass bias behavior of a neighboring element isotope pair is the same as Cu, which is unlikely to be entirely the case.

Secondly, seawater is a particularly challenging sample matrix. Copper concentrations in seawater are extremely low compared to many other elements (e.g., Na, Mg) and Cu is ubiquitously complexed to strong, refractory organic ligands (Bruland et al., 2013). The ability to obtain reliable dissolved Cu concentrations was the subject of a recent study (Posacka et al., 2017), which was motivated by the observation that UV oxidation of acidified seawater samples can lead to an increase in Cu concentrations even in samples stored acidified for extended periods (Achterberg et al., 2001; Biller and Bruland, 2012; Middag et al., 2015; Milne et al., 2010; Posacka et al., 2017; Rapp et al., 2017). Posacka et al. (2017) demonstrate that changes in labile Cu in acidified samples after UV oxidation depend strongly on sample storage time, suggesting that UV oxidation is ineffective with storage times < 2 weeks, is critical for samples stored for ≤3 months, and may be unnecessary with storage times more than ~4 years.

Fig. 2 compares Cu concentrations for Station 18 obtained by the two different methods utilised in this study. The higher resolution dissolved Cu concentration profile was obtained by isotope dilution at NOCS and included 4 h of UV irradiation, while the ETH Zürich isotope samples were stored acidified for ≥4 years, but not irradiated. Good agreement is generally observed for the two profiles at Station 18, given the less precise beam matching approach to Cu concentrations for the isotope analyses. However, at this and other stations, isotope sample concentrations are up to ~30% lower than those measured via the UV-ID-technique, particularly in the water depth range of ~1.5–3 km and in the upper few hundred meters of the water column at Stations 12 and 21 (Fig. S3). It is unclear exactly what effect this lower extraction efficiency (assuming that this is the cause of the lower Cu concentrations for some isotope samples) may have on measured Cu isotope values. However, the fact that seawater δ^{65}Cu is very homogeneous with depth

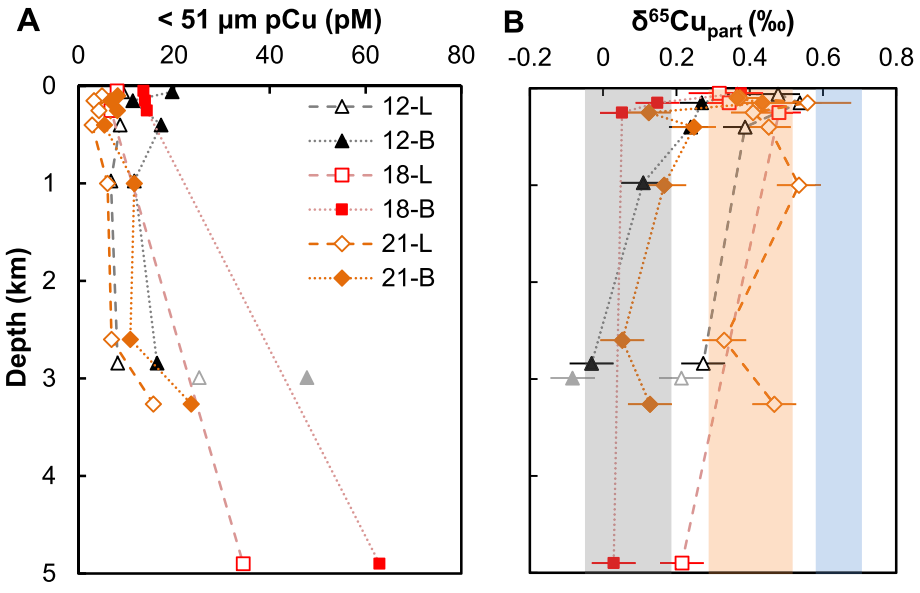

Fig. 7. Bulk (B – filled symbols) and Leachable (L – open symbols) fine-fraction (< 51 μm) particulate (A) Cu concentrations (pCu) and (B) Cu isotope values ($\delta^{65}Cu_{part}$) from SAPS samples at Station 12 (MAR), 18 (deep Argentine basin) and 21 (Argentine slope). Deepest sample at station 12 (greyed out triangles) is considered contaminated based on comparison with bottle filtration data (Fig. 6, see text for discussion). Error bars on isotope values are the long-term reproducibility of a secondary standard (± 0.06‰) or, where larger, the internal 2-sigma uncertainty. In (B), the grey bar represents typical range for lithogenic $\delta^{65}Cu_{lith}$ (Moynier et al., 2017), the blue bar the approximate $\delta^{65}Cu_{seawater}$ observed in the South Atlantic (this study), and the orange bar the range of $\delta^{65}Cu_{auth}$ in bioauthigenic sediments (FeMn crusts and organic rich sediments; Albarède, 2004; Little et al., 2014a, 2017). (For interpretation of the references to colour in this figure legend, the reader is referred to the web version of this article.)

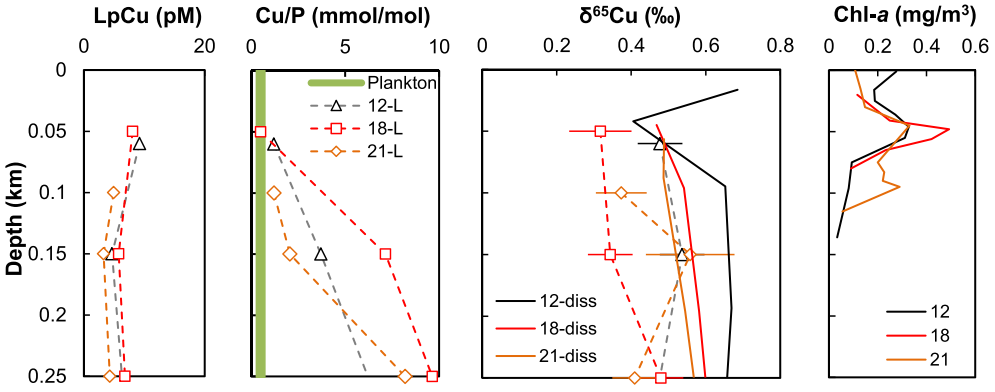

Fig. 8. From left: Upper 250 m leachable particulate Cu concentrations (< 51 μm); leachable particulate Cu/P ratios compared to published range for marine phytoplankton (green bar; range 0.18–0.78: Martin and Knauer, 1973; Collier and Edmond, 1984; Kuss and Kremling, 1999; Ho et al., 2003); leachable particulate δ^{65}Cu (symbols, dashed lines), compared to dissolved phase δ^{65}Cu (solid lines); chlorophyll-*a* concentrations (Wyatt et al., 2014). Nb. *All particulate data from SAPS < 51 μm fine size fraction.* (For interpretation of the references to colour in this figure legend, the reader is referred to the web version of this article.)

and between stations, and for samples with apparently 'good' and 'poor' extraction, implies that any such effect may be slight.

In this context, it is worth reviewing previously published seawater δ^{65}Cu data. The first, pioneering, seawater δ^{65}Cu data was produced using Mg co-precipitation and sample-standard bracketing (Bermin et al., 2006; Vance et al., 2008). Samples from the Indian and Pacific Oceans had been stored acidified for on the order of 10 years, and span δ^{65}Cu = +0.9 to +1.5‰ (Bermin et al., 2006; Vance et al., 2008). They stand out as isotopically heavier than any more recently collected, GEOTRACES-era data, however. This includes data from the Japanese (Nobias resin, Zn-doping with ^{68}Zn/^{66}Zn; no UV, storage time unknown; Takano et al., 2013, 2014, 2017) and Australian (solvent extraction, Ni-doping with ^{62}Ni/^{60}Ni; UV tested and no effect observed, storage time unknown; Thompson et al., 2013; Thompson and Ellwood, 2014) groups, and from this study (Nobias resin, standard-sample bracketing; no UV, storage time ≥ 4 years). These latter studies indicate that the deep ocean has a rather homogeneous δ^{65}Cu composition of about +0.65‰ (see Section 4.3). Using a new method of Cu extraction using NTA resin and H_2O_2 oxidation, Baconnais et al. (this issue) report a similar deep Atlantic open ocean δ^{65}Cu value of +0.60 ± 0.08‰. Nonetheless, Takano et al. (2014) report one data point for a sample from the South Atlantic D357 cruise (#163, Station 3, 4723 m), at +0.43 ± 0.03‰ (2 SD), that is notably lighter than the analysis of the same sample in this study, at +0.61 ± 0.06‰ (Table 3).

Thus, while some degree of agreement for seawater δ^{65}Cu appears to be emerging, a robust isotopic intercalibration is clearly called for, as proposed by Posacka et al. (2017) for dissolved Cu concentrations. This should include quantification of the potential impact of UV-irradiation, acidification strength, storage time, and different analytical procedures. For example, δ^{65}Cu values are very sensitive to the approach chosen to correct for instrumental mass bias. Correction by ^{68}Zn/^{66}Zn doping (Takano et al., 2013, 2014, 2017) is unusual in that, a priori, it would be preferable to correct with the two masses that are as close as possible to the masses being corrected (i.e. ^{66}Zn/^{64}Zn on ^{65}Cu/^{63}Cu; e.g., Vance and Thirlwall, 2002 for neodymium isotopes). Takano et al. (2017) also modify their original method by doping with higher quantities of Zn (Zn:Cu ratio of 3:1 cf. 2:1 in previous studies), in order to reduce the potential contribution of spectral interferences.

Finally, we return to this issue of lingering uncertainty about the true seawater δ^{65}Cu value (or range) at the end of the discussion (Section 4.4), in the context of the larger scale first order conclusions that can be made about Cu isotopes as a palaeoceanographic tracer.

4.2. Particulate Cu and δ^{65}Cu

4.2.1. The distribution of TpCu

Particulate Cu concentrations in the ocean interior are nearly constant with depth. A priori, constant pCu is consistent with the predictions of a simple 1-D reversible scavenging model, in which the quasi-linear increase of dCu with depth is explained by reversible scavenging on particulate material (Little et al., 2013). However, this 1-D model does not take account of the lateral advection of Cu in water masses that accumulate nutrients with age, or of benthic inputs of Cu (Boyle et al., 1977; Bruland, 1980; Jacquot and Moffett, 2015; Roshan and Wu, 2015, see Section 4.3.3).

Away from the ocean interior, pCu concentrations are significantly elevated in the surface ocean, in the deep ocean (> 4000 m) close to the seafloor, and at localised depths along the continental margins (Fig. 5). Detailed characterisation of the contributing particle types to the observed enrichments in pCu awaits further datasets for other elements. However, deep ocean and basin margin particle enrichments are consistent with previous observations of intense benthic nepheloid layers (BNL) in the Argentine Basin (Gardner et al., 2017), and in the west and north Atlantic (e.g., Biscaye and Eittreim, 1977; Brewer et al., 1976; Gardner et al., 2017; Ohnemus and Lam, 2015). Surface ocean particle enrichments could be driven by atmospheric deposition, but aerosol deposition was low over the course of this sampling cruise (Chance et al., 2015). Alternatively, biological productivity may drive particle enrichments in the upper water column (see also Section 4.3.2). Finally, high pCu concentrations are associated with the low salinity tongue of estuarine water from the Río de la Plata river, which flows into the Argentine Basin at the west of the GA10 section (see also Section 4.3.3, Fig. S4).

4.2.2. Leachable (labile) particulate Cu

The leaching procedures utilised in this study aimed to liberate the reactive (labile) Cu fraction of the particles. This labile fraction is believed to be primarily associated with organic phases (e.g., Balistrieri et al., 1981; Collier and Edmond, 1984; Sawlan and Murray, 1983) or, if present, with Mn or Fe oxide phases (e.g., Sherman and Peacock, 2010). Consistent with an association with organic matter, leachable Cu/P ratios of near-surface particulate matter are close to the published range for marine phytoplankton (Fig. 8; published Cu/P range: 0.18–0.78 mmol/mol; Collier and Edmond, 1984; Ho et al., 2003; Kuss and Kremling, 1999; Martin and Knauer, 1973). In contrast, Cu/Mn ratios in Fe-Mn oxide sediments are of the order 0.005 (Little et al., 2014b), much lower than the leachable Cu/Mn ratios of upper water column samples found here, at 0.08–0.5 (Table 4). It is therefore very likely that metabolic and/or organically scavenged Cu dominates the labile pCu pool.

In the subsurface, Cu/P ratios in the leachable particulate phase increase approximately linearly with depth (Fig. 8, full depth profile Fig. S5). Similar increases with depth in the Cu/C ratio of particles collected from sediment traps from the subtropical northeast Pacific have been attributed to scavenging of Cu (Fischer et al., 1986). The fact that leachable pCu concentrations remain approximately constant with depth in the interior South Atlantic, while Cu/P ratios increase, suggests that Cu released from remineralising organic material is re-adsorbed on residual sinking particulate material, while P is returned to the dissolved phase.

4.2.3. Two pools of $\delta^{65}Cu$ in particulate material

Previous work investigating the Cu isotope composition of marine particles is limited. Sediment trap samples from a depth of 2500 m in the northwest Atlantic were analysed for $\delta^{65}Cu$ values by Maréchal et al. (1999), with absolute values ranging from +0.10 to 0.35‰, and seasonal variation of approximately ± 0.11‰ (1 SD). Thompson and Ellwood (2014) encountered analytical difficulties in producing a small dataset of labile and refractory particulate $\delta^{65}Cu$ values from one site (P1) in the Tasman Sea. They report a range in bulk $\delta^{65}Cu$ values of 0.03‰ to 0.52‰, with no systematic variability with depth (range 30 to 1000 m). In general, the labile phase was isotopically heavier than the refractory pool.

Consistent with these two previous studies, we observe a homogeneous leachable particulate $\delta^{65}Cu$ signature throughout the water column, at +0.40 ± 0.10‰ (n = 16, 1 SD; Fig. 7B). This isotope composition is similar to the authigenic Cu isotope signature of Fe-Mn crusts and nodules (Fig. 7; at +0.3 to +0.5‰, Albarède, 2004; Little et al., 2014b) and to the calculated 'bioauthigenic' (non-lithogenic) Cu fraction in sediments from a wide spectrum of marine settings ($\delta^{65}Cu_{auth}$ = +0.31 ± 0.11‰, 1 SD, n = 43; Little et al., 2017).

The bulk digestion procedure accesses a second, refractory pool of particulate Cu. This fraction is evident in bulk digests from below the euphotic zone, where $\delta^{65}Cu_{bulk}$ are lighter than the labile pool, at +0.11 ± 0.09‰ (n = 10, 1 SD; Fig. 7), similar to the average lithogenic Cu isotope composition (at +0.08 ± 0.17‰; Moynier et al., 2017). By mass balance (given $\delta^{65}Cu_{bulk} \cdot pCu_{bulk} = \delta^{65}Cu_{refractory} \cdot pCu_{refractory} + \delta^{65}Cu_{leach} \cdot pCu_{leach}$), the calculated isotope composition of the refractory pool is −0.04 ± 0.31‰ (n = 15, 1 SD). We hypothesize that this refractory pool of Cu is present in a lithogenic, aluminosilicate phase, as proposed by Thompson and Ellwood (2014).

It is interesting to note that the two pools of Cu present in South Atlantic particulates are comparable to the two pools identified in globally distributed marine sediments (Little et al., 2017). $\delta^{65}Cu$ in sediments can, to first order, be described by mixing between two endmembers, a lithogenic endmember at ~0‰ and a bioauthigenic endmember at ~0.3‰ (Little et al., 2017). By comparison, the average offset between leachable (labile) and bulk (≈refractory) particulate $\delta^{65}Cu$, at water depths > 150 m, is 0.28 ± 0.18‰ (1 SD, n = 9), i.e. identical to the offset observed between the lithogenic and bioauthigenic endmembers in sediments. We return to this observation in Section 4.3.1.

Is the labile particulate Cu isotope signature fixed in the upper water column, or does it continue to equilibrate with the dissolved pool at depth? Increasing Cu/P ratios indicate that scavenging continues throughout the water column, so that the Cu isotope composition of the particles should also continue to evolve. Though sampling resolution is lacking, there is an indication that leachable particulate $\delta^{65}Cu$ shifts towards lighter values in the deeper water column (Fig. 7), diverging from the seawater $\delta^{65}Cu$ composition. The homogeneity of the sedimentary Cu output flux also implies continued equilibration of the particulate and dissolved phase at depth, given significant upper water column $\delta^{65}Cu$ variability (e.g., this study, Takano et al., 2014). Ultimately, answering this question requires further high-resolution particulate and dissolved phase Cu isotope studies.

4.3. The distribution of dissolved Cu and $\delta^{65}Cu$

Several processes have been proposed to contribute to the distribution of dissolved Cu. These include water mass mixing, biological uptake, remineralisation of organic material at depth, (reversible) scavenging on particles, organic complexation, hydrothermal activity, and boundary inputs from the continents via aerosol deposition, riverine, groundwater, or benthic fluxes (e.g., Boyle, 1981; Boyle et al., 1977; Bruland and Franks, 1983; Bruland, 1980; Jacquot and Moffett, 2015; Little et al., 2013; Roshan and Wu, 2015). A detailed discussion of the controls on distribution of dissolved Cu along GA10 is beyond the scope of this paper, and will be the subject of a forthcoming manuscript. Here, we focus on the possible influence of each of these processes on the dissolved distribution of Cu isotopes.

4.3.1. Homogeneous interior oceanic $\delta^{65}Cu$

The deep (> 200 m) South Atlantic Cu isotope signature observed in this study, at +0.66 ± 0.07‰, is consistent with recently published data from one station in the North Atlantic (BATS, $\delta^{65}Cu_{>200m}$ = +0.65 ± 0.07‰, n = 6, 1 SD; Boyle et al., 2012), several stations in the Indian and Pacific Ocean ($\delta^{65}Cu_{>200m}$ = +0.65 ± 0.08‰, n = 52, 1 SD; Takano et al., 2014) and from three stations in the Tasman Sea ($\delta^{65}Cu_{>200m}$ = +0.70 ± 0.11‰, n = 29, 1 SD; Thompson and Ellwood, 2014). Together, these data indicate that the deep ocean $\delta^{65}Cu$ composition is homogeneous, at about +0.65‰ (though see discussion in Section 4.1), and isotopically heavy compared to average lithogenic Cu (at +0.08 ± 0.17‰, n = 334, 1 SD; Moynier et al., 2017).

Isotopically heavy Cu in the aqueous phase of rivers and seawater has been attributed to preferential organic complexation of the heavy isotope in the dissolved phase (Little et al., 2014a; Ryan et al., 2014; Takano et al., 2014; Thompson and Ellwood, 2014; Vance et al., 2008). For example, Ryan et al. (2014) measured an isotopic fractionation factor $\Delta^{65}Cu_{ligand\text{-}free}$ (where $\Delta^{65}Cu_{a-b} = \delta^{65}Cu_a - \delta^{65}Cu_b$) of 0.44 ± 0.20‰ (n = 3, 1 SD) for NTA, a synthetic ligand with a similar log K to strong natural L1-type ligands (log K_{NTA} = 14.4). Though Cu speciation data for the South Atlantic GA10 section are as yet unpublished, voltammetric methods have indicated strong organic complexation of Cu throughout the water column in the North Pacific (Buck et al., 2012; Moffett and Dupont, 2007), North Atlantic (Jacquot and Moffett, 2015), Tasman Sea (Thompson et al., 2014), and Atlantic sector of the Southern Ocean (Heller and Croot, 2014).

Isotopically heavy Cu in the dissolved pool is complemented by a light counterpart in the particulate phase (Fig. 7; Section 4.2). Two possible scenarios can be invoked to explain this observation. First, an equilibrium isotope fractionation between the scavenging surface and the organically complexed dissolved pool (as first proposed by Vance et al., 2008). Second, an equilibrium isotope fractionation in the aqueous phase between organically complexed, isotopically heavy Cu, and isotopically light free Cu^{2+} (or weakly complexed Cu), with only the latter scavenged to particles with no further isotope fractionation (Little et al., 2017). Distinguishing between these two hypotheses awaits further detailed experimental work. Regardless of the precise mechanisms, the overall outcome is an extremely homogeneous Cu output flux to sediments, at approximately +0.3‰ (Little et al., 2017).

4.3.2. Variable Cu isotope signatures in the surface and subsurface ocean

While the ocean interior is very homogeneous in Cu isotope composition, deviations towards lighter $\delta^{65}Cu$ values are observed in the upper water column of Stations 21, 18, 12 and 6 (between +0.41 to 0.49‰), and towards heavier $\delta^{65}Cu$ values in the subsurface at stations 3 and 11 (+0.75 and 0.84‰) (Fig. 3). We consider three possible explanations for this upper water column variability: biological activity, aerosol deposition, and local supply followed by mixing from the Río de la Plata estuary.

Copper is an essential nutrient for phytoplankton. In culture, Navarrete et al. (2011) observed that intracellular incorporation by natural consortia of bacteria favours the light Cu isotope, with large metabolically-driven fractionation factors of $\Delta^{65}Cu_{solid\text{-}solution}$ = −1.0 to −4.4‰. Adsorption of Cu by cell surfaces has similarly been shown to favour the light isotope (Navarrete et al., 2011), or to exhibit no fractionation (Pokrovsky et al., 2008). Simultaneously, the free Cu^{2+} ion is toxic at low concentrations to photosynthesizing microorganisms, particularly prokaryotic cyanobacteria (e.g., Brand et al., 1986; Moffett and Brand, 1996). As discussed, these phytoplankton release strong organic ligands that regulate free Cu^{2+} concentrations, with > 99.9%

of dissolved Cu in seawater organically complexed (e.g., Bruland et al., 2013). This complexation is predicted to favour retention of the heavy isotope in solution (Ryan et al., 2014; Sherman, 2013).

On the other hand, eukaryotes (e.g., coccolithophores and diatoms) have higher metabolic Cu requirements than prokaryotes, and appear to be able to access some portion of the ligand-bound Cu pool, possibly via a reductive uptake mechanism (Semeniuk et al., 2009, 2015). If a change in oxidation state facilitates this process (Leal and Van Den Berg, 1998), it could result in stabilisation of isotopically light Cu(I) in surface seawater.

We compare the upper water column dissolved phase data with chlorophyll-*a* concentrations (Fig. 3; Wyatt et al., 2014) and with leachable particulate δ^{65}Cu values (this study, Stations 21, 18 and 12 only; Fig. 8). Note that chlorophyll-*a* concentrations were several orders of magnitude higher in the Cape Basin (Stations 3, 6 and 11) than in the Argentine Basin (Stations 21, 18 and 12), and that the dominant phytoplankton species was estimated to be eukaryotic haptophytes (approx. ~51% of total chlorophyll-*a*; Wyatt et al., 2014).

The deep chlorophyll-*a* maximum (DCM) observed at Stations 3 and 11 (~300 mg m^{-3}) in the Cape Basin correspond to isotopically heavy dissolved Cu (Fig. 3). This would be consistent with preferential uptake of the light isotope alongside active production of organic ligands and complexation of the heavy isotope in the dissolved pool. However, in the Argentine Basin the opposite pattern is observed, notably at Station 12. Here the DCM, which is very low, at ~0.3 mg m^{-3}, is associated with isotopically *light* Cu in the dissolved phase (Figs. 3, 8). This latter pattern, of light Cu isotope values corresponding to the chlorophyll-*a* maximum, has been observed before by Thompson and Ellwood (2014), at Station P1 in the Tasman Sea, and by Takano et al. (2014), at Station BD17 in the northeast Pacific (132.4°W, 43.0°N). However, the fact that it is not a pervasive feature suggests it may be a community specific signature. Browning et al. (2014) predict Station 12 to be Fe limited. Station P1 in the Tasman Sea is oligotrophic and potentially Fe co-limited (Hassler et al., 2014) and the northeast Pacific is also a region of Fe limitation (e.g., Moore et al., 2013). Under Fe-limitation, Cu uptake by phytoplankton is enhanced (Peers and Price, 2006; Semeniuk et al., 2009, 2016). Perhaps this enhanced Cu uptake is manifest in a distinct Cu isotope signature in the aqueous phase. This signature could be envisaged as the result of uptake or scavenging of heavy isotopes by the community growing in situ in the DCM, or to be due to regeneration of isotopically light organic material sinking from above (albeit that the DCM indicates uptake).

In the upper 250 m of the water column in the Argentine Basin, the leachable particulate Cu isotope composition is on average −0.10 ± 0.09‰ (n = 8, 1 SD) lighter than local seawater (Fig. 8; Tables 3, 4), i.e., there appears to be a negligible isotope effect on uptake into plankton or on sorption to organic matter in this region, particularly if there is any contribution of isotopically light Cu to the leachable particulate δ^{65}Cu from the procedural blank (see Section 2.3.1). We note that the residence time of Cu in the dissolved and particulate phases is likely different, however, the negligible isotopic offset between the two pools indicates that there is no strong metabolic control on Cu isotope signatures in the Argentine Basin. It is also consistent with the absence of any relationship between dissolved δ^{65}Cu values and log dCu concentrations across the whole GA10 section (Fig. S6). Thus, while biological activity may drive local variability in upper water column δ^{65}Cu, we suggest that it is not the dominant control.

An alternative mechanism to drive light dissolved δ^{65}Cu in the upper ocean of the Argentine Basin is an external input of isotopically light lithogenic Cu, either from the atmosphere (aerosols) or from the continents. The water-soluble fraction of a small number of aerosols from the North Atlantic CLIVAR A16N section gave δ^{65}Cu = 0.00 ± 0.18‰ (n = 6, 1 SD; Little et al., 2014b), indistinguishable from the lithogenic average. However, atmospheric sources to the Argentine Basin during leg JC068 were minimal (Chance et al., 2015; Wyatt et al., 2014). Furthermore, bulk particulate Cu/Al ratios in the upper 150 m of the water column are $37 \pm 29 \times 10^{-4}$ compared to 3.5×10^{-4} in upper continental crust (Table 4; Rudnick and Gao, 2003). Solubility estimates for lithogenic Cu and Al are of a similar order of magnitude (at about 5–10%; e.g., Baker et al., 2006; Sholkovitz et al., 2010), thus aerosol deposition is unlikely to be responsible for the light Cu isotope signatures observed in the upper water column of this region.

The Río de la Plata estuary is another potential source of lithogenic particles. The Río de la Plata is the second largest drainage basin in South America, after the Amazon, with a hydrographical area of 3,170,000 km^2. Freshwater discharge from the estuary is enriched in macronutrients, dissolved Zn (Wyatt et al., 2014), and dissolved Cu, and exhibits elevated particulate Cu concentrations (Section 4.2.1; Fig. S4). Though we lack Cu isotope data from the region associated with the low salinity tongue of the Río de la Plata, isotopically light Cu signatures at Station 21 and 18 may be consistent with partial dissolution of particulate material in the estuary and mixing of this signal basinwards. Isotopically light Cu has been observed in the particulate phase of a small river in the UK (Vance et al., 2008). Slightly elevated concentrations of Zn in surface ocean of the Argentine Basin have previously been suggested to reflect cross-frontal mixing between the Malvinas Current and Brazil Current (Fig. 1), bringing Zn-enriched waters northward as it flows over the Argentine continental margin (Jullion et al., 2010; Wyatt et al., 2014). Future work should target sampling of the Río de la Plata estuary for trace metal dissolved and particulate phase isotope analyses.

4.3.3. Sedimentary supply of isotopically light Cu to deep waters

Benthic supply of Cu has long been proposed to maintain high dissolved Cu concentrations at depth (Boyle et al., 1977; Bruland, 1980; Jacquot and Moffett, 2015; Posacka et al., 2017; Roshan and Wu, 2015). Pore water studies have suggested a benthic, regenerated source of Cu (Klinkhammer et al., 1982; Klinkhammer, 1980; Widerlund, 1996) and Skrabal et al. (2000) suggest that Cu-binding ligands in pore waters assist this Cu release. Typically, dCu concentrations lack any clear local signature of benthic supply, with smooth correlations observed with, e.g., silicate (Fig. 4; Fig. S7; Jacquot and Moffett, 2015; Roshan and Wu, 2015). Local enrichments in dCu in this South Atlantic dataset (and deviations from the Cu-Si correlation) appear to be related to high TpCu concentrations, associated with local particulate supply from the Río de la Plata estuary and Argentine slope (Fig. S4 and S7).

We do not see clear evidence for scavenging removal of dissolved Cu associated with high particulate concentrations, as seen in some BNLs and overlying the TAG hydrothermal vent field of the MAR in the North Atlantic (Jacquot and Moffett, 2015). We also observe no input of dCu or pCu associated with the MAR in the South Atlantic, suggesting hydrothermal activity does not play a significant role in Cu cycling in this region. A similarly limited role for hydrothermal activity along this section has previously been noted for Zn and Fe (Klunder et al., 2011; Wyatt et al., 2014).

While local dCu enrichments that can be directly tied to benthic input are difficult to identify on a section scale, dissolved phase Cu isotope data appear to be a more sensitive tracer of this process. Several depths along both the east and western margins of the South Atlantic that exhibit localised high pCu concentrations are associated with deviations towards isotopically lighter δ^{65}Cu values in the water column (Fig. 5). At this stage, it is not clear if these isotopically light values reflect supply from pore waters or partial dissolution of the particulate material upon its suspension in and interaction with seawater. The nature of the particulate material is also unknown and awaits further datasets. These are important questions from a whole oceanic mass balance perspective. Copper that is released from the benthic boundary layer on regeneration of organic material (e.g., Klinkhammer et al., 1982; Klinkhammer, 1980) is not a 'new' input of Cu to the ocean, though it may play a role in repartitioning dissolved Cu with depth in the ocean. On the other hand, Cu that may be released from

continentally-derived particulates, or re-released from particles that originated in hydrothermal plumes, would reflect a different source of Cu to those that have so far been characterised isotopically, namely, rivers and aerosols (Little et al., 2014b). We return to these broader issues in the next section.

4.4. Broader paleoceanographic implications

Our best estimate to date of the Cu isotope composition of seawater, at about +0.65‰ (though see Section 4.1) is similar to the discharge-weighted riverine input value, of +0.68‰ (Vance et al., 2008), and to the calculated combined riverine and atmospheric Cu source of +0.63‰ (Little et al., 2014b). However, the steady state oceanic mass balance model of Little et al. (2014b, updated in Little et al., 2017) is out of balance, with a projected isotopically light missing source of Cu (at ~0‰) that is of similar magnitude to the combined riverine and atmospheric flux (Little et al., 2017). Put another way, at steady state, the isotope composition of seawater ($\delta_{seawater}$) can be expressed as:

$$\delta_{seawater} = \delta_{sources} - \Delta_{sinks}$$

where $\delta_{sources}$ is the isotope composition of the sources and Δ_{sinks} is the isotope fractionation on removal of the element from seawater into sediments (the sinks). In the case of Cu, Δ_{sinks} is remarkably consistent across different sedimentary settings, at approximately −0.35‰ (Little et al., 2017). Thus, given a seawater value of +0.65‰, $\delta_{sources}$ must sum up to about +0.3‰, considerably lighter than the input fluxes characterised to date (at about +0.6‰; Little et al., 2014b).

Little et al. (2017) suggest two possible poorly or unconstrained isotopically light sources of Cu: (1) hydrothermal input and (2) partial dissolution of continentally derived particulates. Alternatively, Takano et al. (2014) propose a larger aerosol deposition flux than that suggested by Little et al. (2014b). Our study provides dissolved phase evidence for a particulate-associated flux of isotopically light Cu, both from continental slopes and a large estuary. As noted previously, for this flux to balance the budgetary requirements the Cu released must be derived from continental (or hydrothermal) particulates, and not simply regenerated Cu scavenged on organic (or Fe-Mn oxide) material. Though it is not possible to say with certainty that this is the case based solely on the data presented here, it is plausible. Future pore water and estuarine work should help resolve this question.

Finally, we note that the above discussion is valid even in light of the residual uncertainty surrounding the true seawater δ^{65}Cu value (Section 4.1). If the dissolved pool is, in fact, isotopically heavier than the +0.65‰ estimated here, the mass balance problem is further exaggerated.

5. Conclusions

We present dissolved and particulate phase Cu concentration and Cu isotope data from the South Atlantic UK-GEOTRACES section GA10. This merging of several datasets provides powerful insights into the biogeochemical cycling of Cu, which will only be enhanced by comparison to future datasets for other trace metals and their isotopes in both the dissolved and particulate phase.

Copper is analytically challenging due to its strong organic complexation in seawater and because it has only two stable isotopes, the latter making a double-spike approach to its isotope analysis impossible. We address these issues in the context of a review of published data, and call for a robust laboratory intercalibration of dissolved phase Cu and δ^{65}Cu.

We observe two pools of Cu isotopes in the particulate phase, a refractory pool with a lithogenic δ^{65}Cu signature (at about 0‰) and a labile pool, associated with organic matter, at about +0.4‰. This labile pool is isotopically light compared to the homogeneous deep ocean dissolved pool, the latter being about +0.7‰. We interpret this offset to reflect preferential organic complexation of the heavy isotope in the dissolved phase and scavenging of the light isotope to particles. The fractionation mechanism may be an equilibrium fractionation between the organic ligand bound pool and scavenging surface, or in the aqueous phase, between an organic ligand bound pool and a particle reactive, free Cu^{2+} pool.

Locally, in both surface and deep waters along the continental slopes, we observe deviations towards isotopically light Cu in the dissolved phase. These deviations correspond to enrichments in particulate Cu concentrations, supplied either via sediment resuspension or, in the west, from the Río de la Plata estuary. Copper isotopes appear to trace the previously hypothesized benthic supply route for Cu to the deep ocean.

Finally, we suggest than the supply of isotopically light Cu from sediments and hydrothermal or estuarine particulates may help to balance the oceanic Cu cycle, which is currently missing an isotopically light source of Cu. Future work should test this hypothesis via detailed work in estuaries and in pore waters, and via continued measurement of Cu isotopes in the water column at higher resolution.

Supplementary data to this article can be found online at https://doi.org/10.1016/j.chemgeo.2018.07.022.

Acknowledgements

SHL is supported by a NERC Independent Research Fellowship (NE/P018181/1) and acknowledges prior support from a Leverhulme Trust Early Career Fellowship (ECF-2014-615). We are extremely thankful to Gideon Henderson and all the scientists on both legs of the UK-GEOTRACES GA10 section (D357 and JC068), and to NERC for funding the UK-GEOTRACES program (NE/H00475/1). We are also grateful to two anonymous reviewers and the guest editor Tristan Horner for comments that improved the manuscript.

References

Achterberg, E.P., Braungardt, C.B., Sandford, R.C., Worsfold, P.J., 2001. UV digestion of seawater samples prior to the determination of copper using flow injection with chemiluminescence detection. Anal. Chim. Acta 440, 27–36. https://doi.org/10.1016/S0003-2670(01)00824-8.

Albarède, F., 2004. The stable isotope geochemistry of copper and zinc. Rev. Mineral. Geochem. 55, 409–427. https://doi.org/10.2138/gsrmg.55.1.409.

Anderson, R.F., Hayes, C.T., 2015. Characterizing marine particles and their impact on biogeochemical cycles in the GEOTRACES program. Prog. Oceanogr. 133, 1–5. https://doi.org/10.1016/j.pocean.2014.11.010.

Archer, C., Vance, D., 2004. Mass discrimination correction in multiple-collector plasma source mass spectrometry: an example using Cu and Zn isotopes. J. Anal. At. Spectrom. 19, 656. https://doi.org/10.1039/b315853e.

Asael, D., Matthews, A., Bar-Matthews, M., Halicz, L., 2007. Copper isotope fractionation in sedimentary copper mineralization (Timna Valley, Israel). Chem. Geol. 243, 238–254. https://doi.org/10.1016/j.chemgeo.2007.06.007.

Baconnais I., Rouxel O., Dulaquais G., Boyé M., Determination of the copper isotope composition of seawater revisited: a case study from the Mediterranean Sea (under review, Chemical Geology).

Baker, A.R., Jickells, T.D., Witt, M., Linge, K.L., 2006. Trends in the solubility of iron, aluminium, manganese and phosphorus in aerosol collected over the Atlantic Ocean. Mar. Chem. 98, 43–58. https://doi.org/10.1016/j.marchem.2005.06.004.

Balistrieri, L., Brewer, P.G., Murray, J.W., 1981. Scavenging residence times of trace metals and surface chemistry of sinking particles in the deep ocean. Deep Sea Res. Part A 28, 101–121. https://doi.org/10.1016/0198-0149(81)90085-6.

Berger, C.J.M., Lippiatt, S.M., Lawrence, M.G., Bruland, K.W., 2008. Application of a chemical leach technique for estimating labile particulate aluminum, iron, and manganese in the Columbia River plume and coastal waters off Oregon and Washington. J. Geophys. Res. 113, C00B01. https://doi.org/10.1029/2007JC004703.

Bermin, J., Vance, D., Archer, C., Statham, P.J., 2006. The determination of the isotopic composition of Cu and Zn in seawater. Chem. Geol. 226, 280–297. https://doi.org/10.1016/j.chemgeo.2005.09.025.

Biller, D.V., Bruland, K.W., 2012. Analysis of Mn, Fe, Co, Ni, Cu, Zn, Cd, and Pb in seawater using the Nobias-chelate PA1 resin and magnetic sector inductively coupled plasma mass spectrometry (ICP-MS). Mar. Chem. 130–131, 12–20. https://doi.org/10.1016/j.marchem.2011.12.001.

Biscaye, P.E., Eittreim, S.L., 1977. Suspended particulate loads and transports in the nepheloid layer of the Abyssal Atlantic Ocean. Dev. Sedimentol. 23, 155–172. https://doi.org/10.1016/S0070-4571(08)70556-9.

Bishop, J.K.B., Wood, T.J., 2008. Particulate matter chemistry and dynamics in the twilight zone at VERTIGO ALOHA and K2 sites. Deep-Sea Res. I Oceanogr. Res. Pap. 55,

1684–1706. https://doi.org/10.1016/j.dsr.2008.07.012.
Boyle, E.A., 1981. Cadmium, zinc, copper, and barium in foraminifera tests. Earth Planet. Sci. Lett. 53, 11–35. https://doi.org/10.1016/0012-821X(81)90022-4.
Boyle, E.A., Sclater, F.R., Edmond, J.M., 1977. The distribution of dissolved copper in the Pacific. Earth Planet. Sci. Lett. 37, 38–54. https://doi.org/10.1016/0012-821X(77)90144-3.
Boyle, E.A., John, S., Abouchami, W., Adkins, J.F., Echegoyen-Sanz, Y., Ellwood, M., Flegal, A.R., Fornace, K., Gallon, C., Galer, S., Gault-Ringold, M., Lacan, F., Radic, A., Rehkamper, M., Rouxel, O., Sohrin, Y., Stirling, C., Thompson, C., Vance, D., Xue, Z., Zhao, Y., 2012. GEOTRACES IC1 (BATS) contamination-prone trace element isotopes Cd, Fe, Pb, Zn, Cu, and Mo intercalibration. Limnol. Oceanogr. Methods 10, 653–665. https://doi.org/10.4319/lom.2012.10.653.
Brand, L.E., Sunda, W.G., Guillard, R.R.L., 1986. Reduction of marine phytoplankton reproduction rates by copper and cadmium. J. Exp. Mar. Biol. Ecol. 96, 225–250. https://doi.org/10.1016/0022-0981(86)90205-4.
Brewer, P.G., Spencer, D.W., Biscaye, P.E., Hanley, A., Sachs, P.L., Smith, C.L., Kadar, S., Fredericks, J., 1976. The distribution of particulate matter in the Atlantic Ocean. Earth Planet. Sci. Lett. 32, 393–402. https://doi.org/10.1016/0012-821X(76)90080-7.
Browning, T.J., Bouman, H.A., Moore, C.M., Schlosser, C., Tarran, G.A., Woodward, E.M.S., Henderson, G.M., 2014. Nutrient regimes control phytoplankton ecophysiology in the South Atlantic. Biogeosciences 11, 463–479. https://doi.org/10.5194/bg-11-463-2014.
Browning, T.J., Achterberg, E.P., Rapp, I., Engel, A., Bertrand, E.M., Tagliabue, A., Moore, C.M., 2017. Nutrient co-limitation at the boundary of an oceanic gyre. Nature 551 (7679), 242.
Bruland, L.W., 1980. Oceanographic distributions of cadmium, zinc, nickel and copper in the North Pacific. Earth Planet. Sci. Lett. 47, 176–198.
Bruland, K.W., Franks, R.P., 1983. Mn, Ni, Cu, Zn and Cd in the Western North Atlantic. Trace Met. Sea Water 395–414. https://doi.org/10.1007/978-1-4757-6864-0_23.
Bruland, K.W., Middag, R., Lohan, M.C., 2013. Controls of trace metals in seawater. In: Treatise on Geochemistry: Second Edition, 2nd ed. Elsevier Ltd.. https://doi.org/10.1016/B978-0-08-095975-7.00602-1.
Buck, K.N., Moffett, J., Barbeau, K.A., Bundy, R.M., Kondo, Y., Wu, J., 2012. The organic complexation of iron and copper: an intercomparison of competitive ligand exchange-adsorptive cathodic stripping voltammetry (CLE-ACSV) techniques. Limnol. Oceanogr. Methods 10, 496–515. https://doi.org/10.4319/lom.2012.10.496.
Chance, R., Jickells, T.D., Baker, A.R., 2015. Atmospheric trace metal concentrations, solubility and deposition fluxes in remote marine air over the south-east Atlantic. Mar. Chem. 177, 1–12. https://doi.org/10.1016/j.marchem.2015.06.028.
Chi Fru, E., Rodríguez, N.P., Partin, C.A., Lalonde, S.V., Andersson, P., Weiss, D.J., El Albani, A., Rodushkin, I., Konhauser, K.O., 2016. Cu isotopes in marine black shales record the Great Oxidation Event. Proc. Natl. Acad. Sci. 113, 4941–4946. https://doi.org/10.1073/pnas.1523544113.
Collier, R., Edmond, J., 1984. The trace element geochemistry of marine biogenic particulate matter. Prog. Oceanogr. 13, 113–199. https://doi.org/10.1016/0079-6611(84)90008-9.
Ehrlich, S., Butler, I., Halicz, L., Rickard, D., Oldroyd, A., Matthews, A., 2004. Experimental study of the copper isotope fractionation between aqueous Cu(II) and covellite, CuS. Chem. Geol. 209, 259–269. https://doi.org/10.1016/j.chemgeo.2004.06.010.
Fischer, K., Dymond, J., Lyle, M., Soutar, A., Rau, S., 1986. The benthic cycle of copper: Evidence from sediment trap experiments in the eastern tropical North Pacific Ocean. Geochim. Cosmochim. Acta 50, 1535–1543. https://doi.org/10.1016/0016-7037(86)90327-3.
Gardner, W.D., Mishonov, A.V., Richardson, M.J., 2017. Decadal comparisons of particulate matter in repeat transects in the Atlantic, Pacific and Indian Ocean Basins. Geophys. Res. Lett. 277–286. https://doi.org/10.1002/2017GL076571.
Hassler, C.S., Ridgway, K.R., Bowie, A.R., Butler, E.C.V., Clementson, L.A., Doblin, M.A., Davies, D.M., Law, C., Ralph, P.J., Van Der Merwe, P., Watson, R., Ellwood, M.J., 2014. Primary productivity induced by iron and nitrogen in the Tasman Sea: an overview of the PINTS expedition. Mar. Freshw. Res. 65, 517–537. https://doi.org/10.1071/MF13137.
Heller, M.I., Croot, P.L., 2014. Copper speciation and distribution in the Atlantic sector of the Southern Ocean. Mar. Chem. 173, 253–268. https://doi.org/10.1016/j.marchem.2014.09.017.
Ho, T., Quigg, A., Zoe, V., Milligan, A.J., Falkowski, P.G., Morel, M.M., 2003. The Elemental Composition of Some Marine Phytoplankton 1 Franc. 1159. pp. 1145–1159.
Jacquot, J.E., Moffett, J.W., 2015. Copper distribution and speciation across the International GEOTRACES Section GA03. Deep-Sea Res. II Top. Stud. Oceanogr. 116, 187–207. https://doi.org/10.1016/j.dsr2.2014.11.013.
Jullion, L., Heywood, K.J., Naveira Garabato, A.C., Stevens, D.P., 2010. Circulation and water mass modification in the Brazil–Malvinas Confluence. J. Phys. Oceanogr. 40, 845–864. https://doi.org/10.1175/2009JPO4174.1.
Kagaya, S., Maeba, E., Inoue, Y., Kamichatani, W., Kajiwara, T., Yanai, H., Saito, M., Tohda, K., 2009. A solid phase extraction using a chelate resin immobilizing carboxymethylated pentaethylenehexamine for separation and preconcentration of trace elements in water samples. Talanta 79, 146–152. https://doi.org/10.1016/j.talanta.2009.03.016.
Klinkhammer, G.P., 1980. Early diagenesis in sediments from the eastern equatorial Pacific, II. Pore water metal results. Earth Planet. Sci. Lett. 49, 81–101. https://doi.org/10.1016/0012-821X(80)90151-X.
Klinkhammer, G., Heggie, D.T., Graham, D.W., 1982. Metal diagenesis in oxic marine sediments. Earth Planet. Sci. Lett. 61, 211–219. https://doi.org/10.1016/0012-821X(82)90054-1.
Klunder, M.B., Laan, P., Middag, R., De Baar, H.J.W., van Ooijen, J.C., 2011. Dissolved iron in the Southern Ocean (Atlantic sector). Deep-Sea Res. II Top. Stud. Oceanogr. 58, 2678–2694. https://doi.org/10.1016/j.dsr2.2010.10.042.
Kuss, J., Kremling, K., 1999. Particulate trace element fluxes in the deep northeast Atlantic Ocean. Deep-Sea Res. I Oceanogr. Res. Pap. 46, 149–169. https://doi.org/10.1016/S0967-0637(98)00059-4.
Lam, P.J., Twining, B.S., Jeandel, C., Roychoudhury, A., Resing, J.A., Santschi, P.H., Anderson, R.F., 2015. Methods for analyzing the concentration and speciation of major and trace elements in marine particles. Prog. Oceanogr. 133, 32–42. https://doi.org/10.1016/j.pocean.2015.01.005.
Larner, F., Rehkämper, M., Coles, B.J., Kreissig, K., Weiss, D.J., Sampson, B., Unsworth, C., Strekopytov, S., 2011. A new separation procedure for Cu prior to stable isotope analysis by MC-ICP-MS. J. Anal. At. Spectrom. 26, 1627–1632. https://doi.org/10.1039/c1ja10067j.
Leal, M.F.C., Van Den Berg, C.M.G., 1998. Evidence for strong copper (I) complexation by organic ligands in seawater. Aquat. Geochem. 4, 49–75. https://doi.org/10.1023/A:1009653002399.
Little, S.H., Vance, D., Siddall, M., Gasson, E., 2013. A modeling assessment of the role of reversible scavenging in controlling oceanic dissolved Cu and Zn distributions. Glob. Biogeochem. Cycles 27, 780–791. https://doi.org/10.1002/gbc.20073.
Little, S.H., Sherman, D.M., Vance, D., Hein, J.R., 2014a. Molecular controls on Cu and Zn isotopic fractionation in Fe-Mn crusts. Earth Planet. Sci. Lett. 396, 213–222. https://doi.org/10.1016/j.epsl.2014.04.021.
Little, S.H., Vance, D., Walker-Brown, C., Landing, W.M., 2014b. The oceanic mass balance of copper and zinc isotopes, investigated by analysis of their inputs, and outputs to ferromanganese oxide sediments. Geochim. Cosmochim. Acta 125, 673–693. https://doi.org/10.1016/j.gca.2013.07.046.
Little, S.H., Vance, D., McManus, J., Severmann, S., Lyons, T.W., 2017. Copper isotope signatures in modern marine sediments. Geochim. Cosmochim. Acta 212, 253–273. https://doi.org/10.1016/j.gca.2017.06.019.
Maréchal, C., Albarède, F., 2002. Ion-exchange fractionation of copper and zinc isotopes. Geochim. Cosmochim. Acta 66 (9), 1499–1509.
Maréchal, C.N., Télouk, P., Albarède, F., 1999. Precise analysis of copper and zinc isotopic compositions by plasma-source mass spectrometry. Chem. Geol. 156, 251–273. https://doi.org/10.1016/S0009-2541(98)00191-0.
Martin, J.H., Knauer, G.A., 1973. The elemental composition of plankton. Geochim. Cosmochim. Acta 37, 1639–1653. https://doi.org/10.1016/0016-7037(73)90154-3.
Mason, T.F.D., Weiss, D.J., Chapman, J.B., Wilkinson, J.J., Tessalina, S.G., Spiro, B., Horstwood, M.S.A., Spratt, J., Coles, B.J., 2005. Zn and Cu isotopic variability in the Alexandrinka volcanic-hosted massive sulphide (VHMS) ore deposit, Urals, Russia. Chem. Geol. 221, 170–187. https://doi.org/10.1016/j.chemgeo.2005.04.011.
Mcdonnell, A.M.P., Lam, P.J., Lamborg, C.H., Buesseler, K.O., Sanders, R., Riley, J.S., Marsay, C., Smith, H.E.K., Sargent, E.C., Lampitt, R.S., Bishop, J.K.B., 2015. The oceanographic toolbox for the collection of sinking and suspended marine particles. Prog. Oceanogr. 133, 17–31. https://doi.org/10.1016/j.pocean.2015.01.007.
Middag, R., Séférian, R., Conway, T.M., John, S.G., Bruland, K.W., de Baar, H.J.W., 2015. Intercomparison of dissolved trace elements at the Bermuda Atlantic Time Series station. Mar. Chem. 177, 476–489. https://doi.org/10.1016/j.marchem.2015.06.014.
Milne, A., Landing, W., Bizimis, M., Morton, P., 2010. Determination of Mn, Fe, Co, Ni, Cu, Zn, Cd and Pb in seawater using high resolution magnetic sector inductively coupled mass spectrometry (HR-ICP-MS). Anal. Chim. Acta 665, 200–207. https://doi.org/10.1016/j.aca.2010.03.027.
Moffett, J.W., Brand, L.E., 1996. Production of strong, extracellular Cu chelators by marine cyanobacteria in response to Cu stress. Limnol. Oceanogr. 41, 388–395. https://doi.org/10.4319/lo.1996.41.3.0388.
Moffett, J.W., Dupont, C., 2007. Cu complexation by organic ligands in the sub-arctic NW Pacific and Bering Sea. Deep-Sea Res. I Oceanogr. Res. Pap. 54, 586–595. https://doi.org/10.1016/j.dsr.2006.12.013.
Moore, C.M., Mills, M.M., Arrigo, K.R., Berman-Frank, I., Bopp, L., Boyd, P.W., Galbraith, E.D., Geider, R.J., Guieu, C., Jaccard, S.L., Jickells, T.D., La Roche, J., Lenton, T.M., Mahowald, N.M., Marañón, E., Marinov, I., Moore, J.K., Nakatsuka, T., Oschlies, A., Saito, M.A., Thingstad, T.F., Tsuda, A., Ulloa, O., 2013. Processes and patterns of oceanic nutrient limitation. Nat. Geosci. 6, 701–710. https://doi.org/10.1038/ngeo1765.
Mountain, B.W., Seward, T.M., 1999. The hydrosulphide/sulphide complexes of copper (I): experimental determination of stoichiometry and stability at 22°C and reassessment of high temperature data. Geochim. Cosmochim. Acta 63, 11–29. https://doi.org/10.1016/S0016-7037(98)00288-9.
Moynier, F., Vance, D., Fujii, T., Savage, P., 2017. The Isotope Geochemistry of Zinc and Copper. Rev. Mineral. Geochem. 82, 543–600. https://doi.org/10.2138/rmg.2017.82.13.
Navarrete, J.U., Borrok, D.M., Viveros, M., Ellzey, J.T., 2011. Copper isotope fractionation during surface adsorption and intracellular incorporation by bacteria. Geochim. Cosmochim. Acta 75, 784–799.
Ohnemus, D.C., Lam, P.J., 2015. Cycling of lithogenic marine particles in the US GEOTRACES North Atlantic transect. Deep-Sea Res. II Top. Stud. Oceanogr. 116, 283–302. https://doi.org/10.1016/j.dsr2.2014.11.019.
Ohnemus, D.C., Auro, M.E., Sherrell, R.M., Lagerström, M., Morton, P.L., Twining, B.S., Rauschenberg, S., Lam, P.J., 2014. Laboratory intercomparison of marine particulate digestions including Piranha: a novel chemical method for dissolution of polyethersulfone filters. Limnol. Oceanogr. Methods 12, 530–547. https://doi.org/10.4319/lom.2014.12.530.
Paul, M., Van De Flierdt, T., Rehkämper, M., Khondoker, R., Weiss, D., Lohan, M.C., Homoky, W.B., 2015. Tracing the Agulhas leakage with lead isotopes. Geophys. Res. Lett. 42, 8515–8521. https://doi.org/10.1002/2015GL065625.

Peers, G., Price, N.M., 2006. Copper-containing plastocyanin used for electron transport by an oceanic diatom. Nature 441, 341–344. https://doi.org/10.1038/nature04630.
Planquette, H., Sherrell, R.M., 2012. Sampling for particulate trace element determination using water sampling bottles: methodology and comparison to in situ pumps. Limnol. Oceanogr. Methods 10, 367–388. https://doi.org/10.4319/lom.2012.10.367.
Pokrovsky, O.S., Viers, J., Emnova, E.E., Kompantseva, E.I., Freydier, R., 2008. Copper isotope fractionation during its interaction with soil and aquatic microorganisms and metal oxy(hydr)oxides: possible structural control. Geochim. Cosmochim. Acta 72, 1742–1757. https://doi.org/10.1016/j.gca.2008.01.018.
Posacka, A.M., Semeniuk, D.M., Whitby, H., van den Berg, C.M.G., Cullen, J.T., Orians, K., Maldonado, M.T., 2017. Dissolved copper (dCu) biogeochemical cycling in the subarctic Northeast Pacific and a call for improving methodologies. Mar. Chem. 196, 47–61. https://doi.org/10.1016/j.marchem.2017.05.007.
Rapp, I., Schlosser, C., Rusiecka, D., Gledhill, M., Achterberg, E.P., 2017. Automated preconcentration of Fe, Zn, Cu, Ni, Cd, Pb, Co, and Mn in seawater with analysis using high-resolution sector field inductively-coupled plasma mass spectrometry. Anal. Chim. Acta 976, 1–13. https://doi.org/10.1016/j.aca.2017.05.008.
Revels, B.N., Ohnemus, D.C., Lam, P.J., Conway, T.M., John, S.G., 2015. The isotopic signature and distribution of particulate iron in the North Atlantic Ocean. Deep-Sea Res. II Top. Stud. Oceanogr. 116, 321–331. https://doi.org/10.1016/j.dsr2.2014.12.004.
Roshan, S., Wu, J., 2015. The distribution of dissolved copper in the tropical-subtropical north Atlantic across the GEOTRACES GA03 transect. Mar. Chem. 176, 189–198. https://doi.org/10.1016/j.marchem.2015.09.006.
Rudnick, R.L., Gao, S., 2003. 3.01 - Composition of the continental crust. Treatise Geochem. 1, 1–64. https://doi.org/10.1016/B0-08-043751-6/03016-4.
Ryan, B.M., Kirby, J.K., Degryse, F., Scheiderich, K., McLaughlin, M.J., 2014. Copper isotope fractionation during equilibration with natural and synthetic ligands. Environ. Sci. Technol. 48, 8620–8626. https://doi.org/10.1021/es500764x.
Sawlan, J.J., Murray, J.W., 1983. Trace metal remobilization in the interstitial waters of red clay and hemipelagic marine sediments. Earth Planet. Sci. Lett. 64, 213–230. https://doi.org/10.1016/0012-821X(83)90205-4.
Schlitzer, R., 2016. Ocean Data View.
Semeniuk, D.M., Cullen, J.T., Johnson, W.K., Gagnon, K., Ruth, T.J., Maldonado, M.T., 2009. Plankton copper requirements and uptake in the subarctic Northeast Pacific Ocean. Deep-Sea Res. I Oceanogr. Res. Pap. 56, 1130–1142. https://doi.org/10.1016/j.dsr.2009.03.003.
Semeniuk, D.M., Bundy, R.M., Payne, C.D., Barbeau, K.A., Maldonado, M.T., 2015. Acquisition of organically complexed copper by marine phytoplankton and bacteria in the northeast subarctic Pacific Ocean. Mar. Chem. 173, 222–233. https://doi.org/10.1016/j.marchem.2015.01.005.
Semeniuk, D.M., Taylor, R.L., Bundy, R.M., Johnson, W.K., Cullen, J.T., Robert, M., Barbeau, K.A., Maldonado, M.T., 2016. Iron-copper interactions in iron-limited phytoplankton in the northeast subarctic Pacific Ocean. Limnol. Oceanogr. 61, 279–297. https://doi.org/10.1002/lno.10210.
Sherman, D.M., 2013. Equilibrium isotopic fractionation of copper during oxidation/reduction, aqueous complexation and ore-forming processes: Predictions from hybrid density functional theory. Geochim. Cosmochim. Acta 118, 85–97. https://doi.org/10.1016/j.gca.2013.04.030.
Sherman, D.M., Peacock, C.L., 2010. Surface complexation of Cu on birnessite (δ-MnO_2): Controls on Cu in the deep ocean. Geochim. Cosmochim. Acta 74, 6721–6730. https://doi.org/10.1016/j.gca.2010.08.042.
Sholkovitz, E.R., Sedwick, P.N., Church, T.M., 2010. On the fractional solubility of copper in marine aerosols: toxicity of aeolian copper revisited. Geophys. Res. Lett. 37, 2–5. https://doi.org/10.1029/2010GL044817.
Skrabal, S.A., Donat, J.R., Burdige, D.J., 2000. Pore water distributions of dissolved copper and copper-complexing ligands in estuarine and coastal marine sediments. Geochim. Cosmochim. Acta 64, 1843–1857. https://doi.org/10.1016/S0016-7037(99)00387-7.
Sohrin, Y., Urushihara, S., Nakatsuka, S., Kono, T., Higo, E., Minami, T., Norisuye, K., Umetani, S., 2008. Multielemental determination of GEOTRACES key trace metals in seawater by ICPMS after preconcentration using an ethylenediaminetriacetic acid chelating resin. Anal. Chem. 80, 6267–6273. https://doi.org/10.1021/ac800500f.
Takano, S., Tanimizu, M., Hirata, T., Sohrin, Y., 2013. Determination of isotopic composition of dissolved copper in seawater by multi-collector inductively coupled plasma mass spectrometry after pre-concentration using an ethylenediaminetriacetic acid chelating resin. Anal. Chim. Acta 784, 33–41. https://doi.org/10.1016/j.aca.2013.04.032.
Takano, S., Tanimizu, M., Hirata, T., Sohrin, Y., 2014. Isotopic constraints on biogeochemical cycling of copper in the ocean. Nat. Commun. 5, 5663.
Takano, S., Tanimizu, M., Hirata, T., Sohrin, Y., 2015. Isotopic constraints on biogeochemical cycling of copper in the ocean. Nat. Commun. 5, 1–7. https://doi.org/10.1038/ncomms6663.
Takano, S., Tanimizu, M., Hirata, T., Shin, K.C., Fukami, Y., Suzuki, K., Sohrin, Y., 2017. A simple and rapid method for isotopic analysis of nickel, copper, and zinc in seawater using chelating extraction and anion exchange. Anal. Chim. Acta 967, 1–11. https://doi.org/10.1016/j.aca.2017.03.010.
Thompson, C.M., Ellwood, M.J., 2014. Dissolved copper isotope biogeochemistry in the Tasman Sea, SW Pacific Ocean. Mar. Chem. 165, 1–9. https://doi.org/10.1016/j.marchem.2014.06.009.
Thompson, C.M., Ellwood, M.J., Wille, M., 2013. A solvent extraction technique for the isotopic measurement of dissolved copper in seawater. Anal. Chim. Acta 775, 106–113. https://doi.org/10.1016/j.aca.2013.03.020.
Thompson, C.M., Ellwood, M.J., Sander, S.G., 2014. Dissolved copper speciation in the Tasman Sea, SW Pacific Ocean. Mar. Chem. 164, 84–94. https://doi.org/10.1016/j.marchem.2014.06.003.
Tuerena, R.E., Ganeshram, R.S., Geibert, W., Fallick, A.E., Dougans, J., Tait, A., Henley, S.F., Woodward, E.M.S., 2015. Nutrient Cycling in the Atlantic Basin: The Evolution of Nitrate Isotope Signatures in Water Masses. pp. 1830–1844. https://doi.org/10.1002/2015GB005164.
Twining, B.S., Rauschenberg, S., Morton, P.L., Ohnemus, D.C., Lam, P.J., 2015a. Comparison of particulate trace element concentrations in the North Atlantic Ocean as determined with discrete bottle sampling and in situ pumping. Deep-Sea Res. II Top. Stud. Oceanogr. 116, 273–282. https://doi.org/10.1016/j.dsr2.2014.11.005.
Twining, B.S., Rauschenberg, S., Morton, P.L., Vogt, S., 2015b. Metal contents of phytoplankton and labile particulate material in the North Atlantic Ocean. Prog. Oceanogr. 137, 261–283. https://doi.org/10.1016/j.pocean.2015.07.001.
Vance, D., Thirlwall, M., 2002. An assessment of mass discrimination in MC-ICPMS using Nd isotopes. Chem. Geol. 185, 227–240.
Vance, D., Archer, C., Bermin, J., Perkins, J., Statham, P.J., Lohan, M.C., Ellwood, M.J., Mills, R.A., 2008. The copper isotope geochemistry of rivers and the oceans. Earth Planet. Sci. Lett. 274, 204–213. https://doi.org/10.1016/j.epsl.2008.07.026.
Vance, D., Little, S.H., Archer, C., Cameron, V., Andersen, M.B., Rijkenberg, M.J.A., Lyons, T.W., 2016. The oceanic budgets of nickel and zinc isotopes: the importance of sulfidic environments as illustrated by the Black Sea. Philos. Trans. R. Soc. A Math. Phys. Eng. Sci. 374, 20150294. https://doi.org/10.1098/rsta.2015.0294.
Widerlund, A., 1996. Early diagenetic remobilization of copper in near-shore marine sediments: a quantitative pore-water model. Mar. Chem. 54, 41–53. https://doi.org/10.1016/0304-4203(96)00024-2.
Wyatt, N.J., Milne, A., Woodward, E.M.S., Rees, A.P., Browning, T.J., Bouman, H.A., Worsfold, P.J., Lohan, M.C., 2014. Biogeochemical cycling of dissolved zinc along the GEOTRACES South Atlantic transect GA10 at 40°S. Glob. Biogeochem. Cycles 28, 44–56. https://doi.org/10.1002/2013GB004637.
Yeats, P.A., Westerlund, S., Flegal, A.R., 1995. Cadmium, copper and nickel distributions at four stations in the eastern central and south Atlantic. Mar. Chem. 49 (4), 283–293.
Zhu, X.K., Guo, Y., Williams, R.J.P., O'Nions, R.K., Matthews, A., Belshaw, N.S., Canters, G.W., de Waal, E.C., Weser, U., Burgess, B.K., Salvato, B., 2002. Mass fractionation processes of transition metal isotopes. Earth Planet. Sci. Lett. 200, 47–62. https://doi.org/10.1016/S0012-821X(02)00615-5.